

AN ABSTRACT OF THE THESIS OF

Jessica Grace Cawley for the degree of Master of Science in Civil Engineering presented on March 20, 2014.

Title: Review of Guidelines for the Design of Tsunami Vertical Evacuation Buildings

Abstract approved:

Andre R. Barbosa

Harry H. Yeh

Tsunamis have the potential to inflict severe damage and loss of life in coastal communities. Structures known as vertical evacuation buildings provide an alternative evacuation site for communities living in relatively flat, coastal regions with inadequate sources of high ground for evacuation. Design of these structures balances risk and economy, and requires both technical and social design considerations. The design must be ductile enough to resist seismic vibrations and also strong enough to resist static and hydrodynamic loads and impact forces from floating debris. Uncertainties in the tsunami wave characterization and force determination promote over-conservative designs which may be cost-prohibitive to build. Previous to the March 11, 2011 earthquake and tsunami in Japan, well-engineered reinforced concrete structures were thought to withstand tsunamis; however, in the 2011 event, many engineered reinforced concrete buildings failed as the tsunami forces were greater than anticipated.

In order to properly determine the forces on a structure, the tsunami waves must be adequately characterized; this process is called the Tsunami Hazard Analysis. The key factors used to characterize tsunamis are identified and their imbedded uncertainties are discussed. The Tsunami Hazard Analysis can provide a range of precision in its output values and therefore a tiered approach to the Tsunami Structural Analysis that follows the Tsunami Hazard Analysis is proposed.

In the Tsunami Structural Analysis, the velocity and height parameters characterize the tsunami and are used to determine the actual forces on a structure. Three

tiers have been provided based on the information available for the site based on the tsunami hazard assessment: Tier 1 includes only runup elevation or height parameters of the tsunami inundation. Tier 2 includes detailed depth and velocity information provided from a numerical model of the area. Tier 3 includes a time series of depth and velocity information and may use a fluid-structure interaction numerical model to determine the forces directly. The first two tiers can be found in various forms in existing guidelines. The third tier is recommended for important facilities such as tsunami vertical evacuation buildings.

The existing methodologies in the guidelines for the design of Vertical Evacuation Buildings, such as FEMA P-646, are reviewed. Their advantages, uncertainties, and limitations in the context of the discussions on Tsunami Hazard Assessment and Tsunami Structural Analysis are discussed. Based on the findings of this research, a tiered design rationale is proposed in order to clearly categorize uncertainties in the force estimation process. In addition to the rationale, main conclusions of this research include: (1) tsunami parameter clarification, including assumptions/applicability of different depth, velocity, added mass coefficients, among other parameters; (2) identification of need for flow parameter $(h^2u^2)_{\max}$ for computing overturning moments with reduced uncertainty; (3) building shape effects, for example U-shaped building coefficients need to be developed for the estimation of drag force and also in the determination of realistic and governing tsunami force combinations; and (4) identification and applicability of critical flow conditions as well as appropriate force combinations. The four topics above are important to mitigate risk in the design of vertical tsunami evacuation buildings and to promote economical designs that are feasible for many communities.

© Copyright by Jessica Grace Cawley
March 20, 2014
All Rights Reserved

Review of Guidelines for the Design of Tsunami Vertical Evacuation Buildings

by
Jessica Grace Cawley

A THESIS

submitted to

Oregon State University

in partial fulfillment of
the requirements for the
degree of

Master of Science

Presented March 20, 2014
Commencement June 2014

Master of Science thesis of Jessica Grace Cawley presented on March 20, 2014.

APPROVED:

Major Professor, representing Civil Engineering

Co-major Professor, representing Civil Engineering

Head of the School of Civil and Construction Engineering

Dean of the Graduate School

I understand that my thesis will become part of the permanent collection of Oregon State University libraries. My signature below authorizes release of my thesis to any reader upon request.

Jessica Grace Cawley, Author

ACKNOWLEDGMENTS

First, I would like to thank God for the abundant grace and provision in my life and in this project. I would also like to thank Dr. Harry Yeh and Dr. Andre Barbosa for mentoring me in the fields of tsunami and structural engineering. Your passion for the profession and for teaching is inspiring. I would like to thank Dr. Miller for all his dedication as a professor and for mentoring myself and countless other students. I would like to thank Dr. Higgins for being so full of character and wit, and for encouraging me to study structural engineering. I would like to thank Cindy Olson for her kindness and encouragement through the years. I hold the highest respect for you all. I would also like to thank my friends and family for all your love and support.

TABLE OF CONTENTS

	<u>Page</u>
1 Introduction	2
1.1 Background.....	2
1.2 Terminology	4
1.3 Objectives	4
1.4 Thesis Overview	5
2 Tsunami Hazard Assessment.....	8
2.1 Tsunami Wave General Description.....	8
2.1.1 Waveform	9
2.1.2 Locally Generated Tsunamis	12
2.1.3 Far-source Generated Tsunamis	14
2.1.4 Wavelengths	14
2.2 Terrain and Local Conditions	15
2.3 Bathymetry	19
2.4 Laboratory Testing	19
3 Tsunami Structural Analysis	20
3.1 Observed Failure Modes.....	20
3.1.1 Overturning	21
3.1.2 Sliding	22
3.2 Definition of “Flow Velocity”	23
3.3 Definition of “Flow Depth”	23
3.4 Surge Front vs. Bore Front	27
3.4.1 Surge.....	27
3.4.2 Bore	28
3.5 Forces.....	29
3.5.1 Hydrodynamic Force	30
3.5.2 Hydrostatic	32
3.5.3 Buoyant Force	34
3.5.4 Impulsive Force	35
3.5.5 Debris Impact	37
3.5.6 Jamming	44

TABLE OF CONTENTS (Continued)

	<u>Page</u>
3.5.7 Maximum Total Force	44
3.5.8 Tsunami Force Combinations	47
3.6 Dimensions, Shape and Orientation	51
3.6.1 U-Shaped Buildings	51
3.6.2 Breakaway Windows/Walls	52
4 Review of Tsunami Vertical Evacuation Building Guidelines	56
4.1 United States	57
4.1.1 Federal Emergency Management Agency, P-646	58
4.1.2 City of Honolulu Building Code (Dames & Moore, 1980)	58
4.1.3 United States Nuclear Regulatory Committee	59
4.2 Japan	59
4.2.1 Cabinet Office Guidelines	60
4.2.2 Ministry of Land, Infrastructure, Transportation and Tourism	62
4.3 Other	62
4.3.1 Palermo, Nistor, Nouri, & Cornett	63
4.3.2 World Bank	63
4.3.3 The World Association for Waterbourne Transport Infrastructure	63
4.4 Conclusion	63
5 Proposed Design Rationale	64
5.1 Tier 1 Analysis	66
5.2 Tier 2 Analysis	67
5.3 Tier 3 Analysis	67
6 Conclusions	70
7 References	73
APPENDIX	78

LIST OF FIGURES

<u>Figure</u>	<u>Page</u>
Figure 1-1: Tsunami Design Terminology Adapted from: (Chock, 2012a).....	4
Figure 1-2: Design Rationale for Tsunami Vertical Evacuation Buildings	6
Figure 2-1: Waveforms and Theoretical Runup Laws (Geist, 1999)	9
Figure 2-2: Tide gage records for the 2004 Indian Ocean tsunami (Yeh, 2009) (Digitized by Robertson, 2007)	11
Figure 2-3: Wave propagation of 2004 Indian Ocean Tsunami (NASA, 2005)	12
Figure 2-4: Schematic diagrams of the vertical displacement resulting from subduction-type fault dislocation. Source: (Geist, 1999)	13
Figure 2-5: Sea level records of tsunami waves at four locations in British Columbia on March 27-29, 1964 (Thomson, 1981; Wigen & White, 1964)	16
Figure 2-6: Resonance in Port Alberni, Canada (Wigen & White, 1964).....	17
Figure 2-7: Channeling Effects in Callao, Peru (Photo courtesy of Harry Yeh).....	18
Figure 3-1: Height & Velocity Relationship Sketch (Source: Asakura, 2002)	22
Figure 3-2: Tsunami Design Terminology Adapted from: (Chock, 2012)	24
Figure 3-3: Over-conservative Inundation (Adapted from FEMA P-646, 2012).....	25
Figure 3-4: Well-predicted Inundation (Adapted from FEMA P-646, 2012)	26
Figure 3-5: Under-predicted Inundation (Adapted from FEMA P-646, 2012)	26
Figure 3-6: Surge Definition Sketch (Keulegan, 1950).....	27
Figure 3-7: Hydraulic Jump - Bore Front Analogy (Mohamed, 2008)	29
Figure 3-8: Hydrodynamic Force Assumption	31
Figure 3-9: Stages of Hydrostatic Force Application on a Global Scale	33
Figure 3-10: Empirical Relationship of Impulsive Force to the Hydrodynamic Force (Arnason et al., 2009)	35
Figure 3-11: Debris Impact Force (Courtesy of Andre R. Barbosa)	38
Figure 3-12: Spring System Assumption	41

LIST OF FIGURES (Continued)

<u>Figure</u>	<u>Page</u>
Figure 3-13: Orientation of Impact (Haehnel & Daly, 2002a)	43
Figure 3-14: Hypothetical Total Force Time Series for Rectangular Structure	46
Figure 3-15: Hypothetical Total Force Time Series for U-shaped Structure	47
Figure 3-16: Scenario 1 Proposed by FEMA P-646	48
Figure 3-17: Scenario 2 Proposed by FEMA P-646	48
Figure 3-18: Scenario 3 Proposed by FEMA P-646	49
Figure 3-19: Hydrodynamic Force Application – Elevation View	50
Figure 3-20: “U-Shaped” Building	51
Figure 3-21: Example of Breakaway Walls in Rikuzpa-Takata, Japan (Photo courtesy of Harry Yeh)	53
Figure 3-22: Effects of Openings on a Structure. Data Source: Lukkunaprasit (2008)	54
Figure 4-1: Example of Significant Variation of Runup Heights: 1993 Okushiri Tsunami (Source: Yeh, 2009)	57
Figure 4-2: Asakura (2002) Model Definition Estimating Total Tsunami Force	61
Figure 5-1: Design Rationale for Tsunami Vertical Evacuation Buildings	64
Figure 5-2: Tiered Approach to Tsunami Force Estimation	65

LIST OF TERMS

Depth Parameters:

η_{max}	Maximum inundation depth at the site of interest
d_s	Water depth of the surge head immediately behind the surge front
h_b	Flow depth behind the bore front
hu^2	Flow depth causing the maximum value of the momentum flux
h^2u^2	Flow depth causing the maximum moment at the base
<i>not specified</i>	Flow depth of maximum velocity, exceeding depth of debris draft
h_j	Height of a bore impinging upon still-water
h_s	Quiescent water depth in front of the advancing bore
h_b	Combination of quiescent water depth and bore height
H	Water depth of the reservoir in a dam break scenario
R	Elevation above mean sea-level of the furthest location of inundation
z	Ground elevation of the location of interest
y	Height above ground level of a specific location on a building

Velocity Parameters:

u_0	Velocity of a surge
c	Bore propagation speed /wave speed
u_j	Velocity of bore front
u	Combined flow velocity

Review of Guidelines for the Design of Tsunami Vertical Evacuation Buildings

by
Jessica Grace Cawley

1 INTRODUCTION

Tsunamis pose an extreme hazard to human life. Over 300,000 lives were lost in the 13 nations affected by the December 2004 Indian Ocean Tsunami (Phillips, Neal, Wikle, Subanthore, & Hyrapiet, 2008). In 2011, a magnitude Mw 9.0 earthquake struck the coast of Japan's Tohoku region causing catastrophic damage together with the loss of 15,883 lives, and 2,654 people are still missing three years later (National Police Agency of Japan, 2014). Therefore, in a strive towards building tsunami resilient communities, engineers, and scientists have focused their research on the development of life saving mitigation strategies, such as creating early warning systems and effective evacuation routes.

High ground is the safest place to go during a tsunami, however, when insufficient time and geographical conditions prevent evacuation to high ground, an alternative that has been proposed and implemented in several areas of the world is a Tsunami Vertical Evacuation Building. FEMA P-646 (2012) shows some examples of tsunami vertical evacuation buildings in Japan, typically made of reinforced concrete. Man-made earthen berms are also used as a place for tsunami evacuation. An evacuation berm in the Sendai Port was constructed to a height exceeding the inundation height during the 2011 tsunami in Japan (FEMA P-646, 2012). Tsunami evacuation buildings must be capable of withstanding seismic and tsunami loads, and are ideal for situations in which flat topography is prevalent near the shoreline and when high ground is not achievable within reasonable distance and time.

1.1 Background

Until very recently, reinforced-concrete structures engineered to withstand seismic loads were assumed to withstand tsunamis. This assumption did not hold for the Japan, Tohoku, 2011 event; many engineered reinforced concrete buildings failed due to the unexpected magnitude of tsunami forces (Yeh, Sato, & Tajima, 2013). This observation may seem anecdotal, but it becomes of extreme importance as many coastal communities in the Pacific Northwest of the United States (Raskin et al., 2011) have already begun discussing the design, capacity, and the quantity of tsunami evacuation

buildings based on their specific tsunami risks and the resources available to the community. Cascadia subduction zone events are anticipated to have only 10 to 30 minutes of warning time. In coastal towns such as Long Beach, Washington and Seaside, Oregon, it may be very difficult to reach high ground in such a short amount of time, and this difficulty may be compounded by the additional challenge of navigating through people who may be frantic and disoriented from the earthquake. Thus, it is of extreme importance that reliable guidelines allow for design of the next generation of tsunami vertical evacuation buildings that are now being proposed in the US, and that design should be economical to the extent possible without compromising safety.

According to FEMA P-646 (2012), a tsunami vertical evacuation building should possess the following attributes: (i) capable of withstanding tsunami forces and scour; (ii) tall enough to provide dry standing-room for the evacuees; (iii) a public-use building (such as a parking structure); (iv) accessible at all hours of the day; when possible (v) sited away from potential debris sources or other site hazards; (vi) accessible to many people entering at once; and (vii) located away from the shoreline and in the direction of high-ground evacuation. Not only are wave forces and water depths larger near the shoreline, but also people are unlikely to run towards the coast to find shelter in a tsunami vertical evacuation building. Furthermore, and most importantly, people must be aware of the existence of such a building.

Guidelines such as FEMA P-646 (2012) provide a comprehensive review of factors to consider during the design process for tsunami vertical evacuation buildings. In the US, a new version of ASCE 7 is expected to come out soon with some consideration of the estimation of the tsunami forces and load combinations for design of structures susceptible to tsunami forces. Other guidelines, like those from Japan for example, also address the tsunami force estimation procedures and, in some cases, design methodologies are proposed. However, diverse terminology and very different inexplicit or even unexplained assumptions, can lead to uneconomical and even unsafe designs.

1.2 Terminology

One interesting feature of tsunami engineering is that it requires dialog between ocean/coastal engineers and structural engineers. Thus, a common terminology needs to be set such that both specialties can “speak” the same language. The discrepancies in terminology appear in both the tsunami guidelines and research literature.

Figure 1-1 illustrates the main definitions used in this study. The term wave “height” is used to define measured from the tide level at the event of a tsunami as a datum, whereas “elevation” uses the mean sea level as the reference. Moreover, the term “depth” uses the ground surface level as a datum for measurements. This is shown in detail in Figure 1-1.

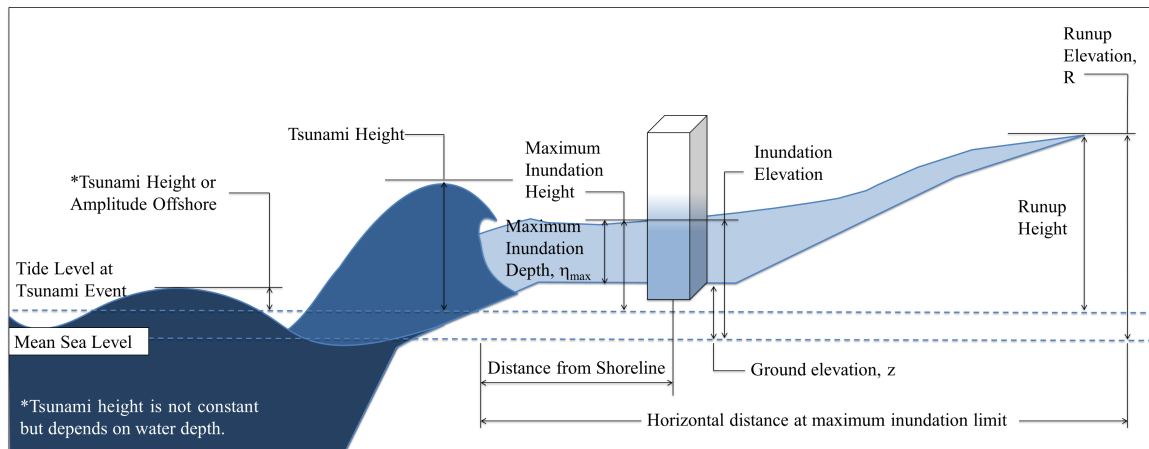


Figure 1-1: Tsunami Design Terminology
Adapted from: (Chock, 2012a)

1.3 Objectives

The main objective of this study is to propose a design rationale that will account for the different levels of uncertainty and explicitly state the assumptions made in the definition of the design loads. While, uncertainty in the earthquake parameters encompass the majority of uncertainty in seismic design and assessments, in tsunami engineering a large uncertainty remains in determination of the flow parameters, debris, and scour, as well as force determination even after the scenario earthquakes are defined. To achieve the main objective of this study, the following tasks were performed:

1. Review basic concepts of tsunami engineering design and clarify/unify terminology from different sources based on physical understanding of the tsunami events.
2. Review critical flow conditions and force combinations.
3. Identify need of a term for computing peak overturning moments, primarily for building stability.
4. Identify the absence and need for building shape effect consideration, especially for U-shaped buildings.
5. Propose a design rationale to reduce uncertainty in design, based on a tiered analysis methodology.

1.4 Thesis Overview

In this study, the presentation of information and discussion follows the proposed design rationale shown in Figure 1-2. The design rationale is divided into three main parts. In the first part, the Tsunami Hazard Analysis, flow conditions are assessed and the quantification of the potential for scour and debris are also considered. In the second part, the Tsunami Structural Analysis, tsunami forces are estimated used to obtain internal forces and displacements. Once the internal demands are estimated, the third and final part of the design rationale follows the traditional design verification process for different members using existing structural design provisions.

This thesis focuses on the characterization of “Flow Conditions” within Tsunami Hazard Analysis and the “Tsunami Force Estimation” within the Tsunami Structural Analysis component of the design rationale. In the Tsunami Hazard Analysis, discussions on debris characterization and scour at a site of interest fall outside the scope of this work.

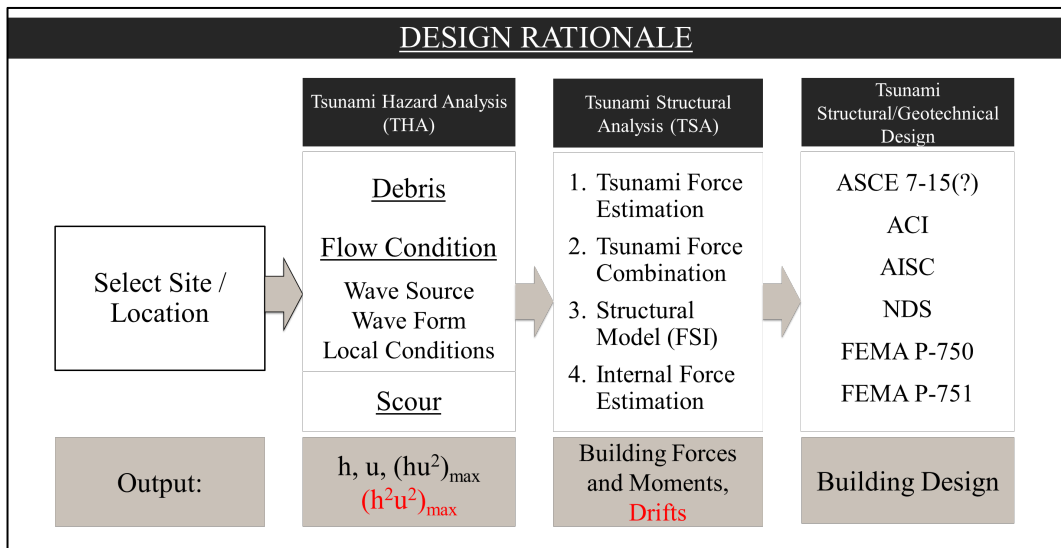


Figure 1-2: Design Rationale for Tsunami Vertical Evacuation Buildings

In Chapter 2, basic concepts for the design of tsunami vertical evacuation buildings are discussed to aid in the understanding of the uncertainty imbedded throughout the force estimation process, starting with flow conditions, local bathymetry and terrain effects, and model waveforms. These influence the flow environment and are ultimately incorporated during the Tsunami Hazard Analysis to produce height and depth parameters which are then used to determine forces. The extreme uncertainty due to local effects requires caution due to the possibility of greatly under-estimating and over-estimating tsunami wave forces on buildings. For example, design guidelines do not currently include wave channeling from the local terrain (Charvet, 2012) nor are provisions made for increases in water depth and velocity due to other standing buildings remaining during the tsunami. Once the flow parameters (depth and height) are determined, forces can be determined.

In Chapter 3, a discussion of tsunami design parameters as they relate to the ultimate structural design of reinforced concrete buildings for the purpose of vertical evacuation buildings is presented. The parameters explained in the tsunami hazard analysis are calibrated to determine forces on typical buildings using (a) only depth, if velocity parameters are not available, or (b) a combination of depth and velocity parameters that require a load combination to determine peak total force. Flow

conditions/force combinations are explained using a method provided in FEMA P-646 (2012); however, recommendations are made herein to improve the determination of total peak tsunami force in order to reduce uncertainty. A need for consideration of non-typical shapes, such as U-shaped buildings, was discovered from extensive surveys of the damage caused by the 2004 Sumatra Earthquake tsunami in the areas of Sri Lanka and Thailand. U-shaped buildings were recorded as having higher total force effects than rectangular or square structures (Okada, Sugano, Ishihara, Takai, & Tateno, 2006). Drag coefficients have been developed to incorporate the shape of a structure, but only for circular and square columns (FEMA CCM, 2003). No coefficient exists for other shapes, such as U-shaped buildings.

In Chapter 4, and in support of the design rationale proposed in Figure 1-2, several existing methodologies are reviewed, including *Guidelines for Design of Structures for Evacuation from Tsunamis* (FEMA P-646, 2012) and the Japanese Guidelines by the Building Center of Japan and the Cabinet Office (Okada et al., 2006). Various other design methodologies are also discussed.

Ultimately, in Chapter 5, a design rationale and three-tiered analysis strategy is proposed. The strategy acknowledges different levels of uncertainty in the design process. The gaps in the body of knowledge are addressed to reduce uncertainty of forces to design both safe and economical buildings in the future.

In summary, the engineering dilemma discussed in this thesis addresses the quest for the safety and welfare of society while balancing the economy of designs. This is difficult, especially in the case of a tsunami, which is an infrequent and unforeseen event in the long term and also of unknown magnitude, making the perceived importance of designing tsunami vertical evacuation buildings highly variable between communities. Tsunami vertical evacuation building designs are not realizable if the design requirements are too conservative and financially infeasible to build; however, it would be a tragedy for such a building to fail to preserve the lives it was intended to protect in the event of a tsunami. The discussion provided herein is written with the hope of clarifying the topic for a broad audience of coastal and structural engineers, exposing uncertainties in design and proposing a design rationale that explicitly accounts for those uncertainties.

2 TSUNAMI HAZARD ASSESSMENT

The following section discusses fundamental principles of understanding tsunami waves and how they are characterized in order to understand how they will runup onto land. The purpose for their inclusion in this report is to identify areas of uncertainty in the Tsunami Hazard Analysis process depending on the specific location of the site of interest. Different wave forms will be briefly discussed since they are the tools used by scientists and engineers to model tsunamis.

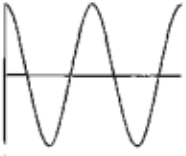

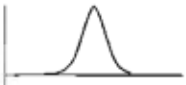
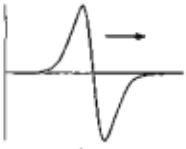
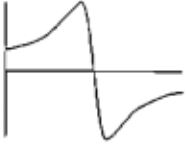
2.1 Tsunami Wave General Description

A tsunami is a wave, or series of waves, generated by underwater earthquake motion, landslides, volcanic eruptions, or even avalanches. This paper focuses on tsunamis generated by earthquakes primarily because it has been reported in the literature that a majority of recorded tsunamis are earthquake-induced tsunamis (e.g. NRC report, 2011). Tsunami source areas are very large for those generated by earthquakes (more than 5000 km²), while the sources created by other mechanisms are relatively small (less than 100 km²). Typically, co-seismically generated tsunamis propagate over long distances only with slight attenuation. As tsunamis approach the coast, and water depth decreases, the wave height increases significantly due to the shoaling effect. When tsunamis reach the shoreline, the tsunami inundates the shore and runup may extend over a few miles inland, depending on topographical conditions of the coastline.

Uncertainties first enter the design process with the estimation of the source earthquake. The National Tsunami Hazard Mitigation Program (NTHMP) is working to produce a credible worst-case scenario (Bernard, 2005). In Oregon, early tsunami inundation maps were produced by modeling one specific earthquake scenario (Priest, 1995). Recently, DOGAMI (2013) has produced inundation maps that model five local-source (Cascadia subduction zone) and two distant-source (Gulf of Alaska subduction zone) tsunamis.

2.1.1 Waveform

Tsunamis cannot be characterized by one specific waveform. Every tsunami has, more or less, a different appearance. Different profiles have been defined for the waveforms, the most common being Boussinesq (a long-wave assumption) solitary waves and N-waves (Tadepalli & Synolakis, 1996). Figure 2-1 shows five common models for wave forms, including a solitary wave and an N-wave, used to theorize runup on a beach.

Waveform	Graph	Run-up law	Reference
Sinusoidal wave		$\frac{R}{H} = [J_0^2(U) + J_1^2(U)]^{-1/2}$ $U = \frac{4\pi d}{L} \cot \beta^{(b)}$	Keller and Keller (1964); Shuto (1972)
Cnoidal wave		see reference	Synolakis et al. (1988)
Solitary wave		$R = 2.83 \sqrt{\cot \beta} H^{5/4(c)}$	Synolakis (1987)
N-wave		$R = 3.86 \sqrt{\cot \beta} H^{5/4(c, d)}$	Tadepalli and Synolakis (1994a)
Lorentz wave		$\frac{R}{H} = P + \sqrt{(d \cot \beta)/L} \quad (e)$ $P = \pi\sqrt{2} \cos^{5/2}(2\theta/5)$	Pelinovsky and Mazova (1992)

^a For each case, R , H , d , and β are the maximum runup, initial wave height, initial water depth, and slope angle, respectively. See references for specific applications and limiting conditions.

^b U notation from Togashi (1983) (see text). L is wavelength. J_0 and J_1 are the zeroth-order and first-order Bessel functions, respectively.

^c Spatial parameters nondimensionalized with respect to the initial water depth (d).

^d Valid for isosceles N-wave. See reference for generalized N-wave runup law.

^e See reference for specific parameters and conditions.

Figure 2-1: Waveforms and Theoretical Runup Laws (Geist, 1999)

2.1.1.1 Solitary Waves

Solitary waves are a waveform used to describe tsunamis that have a single positive surface displacement, whereas N-waves have both a positive and a negative surface displacement, as shown in Figure 3-1. A solitary wave is a wave that propagates in space without variation in shape or size. Using a solitary wave form to characterize a tsunami is typical in experimental studies, as well as analytical and numerical studies. The stable form of the positive surface displacement makes it useful for predicting the runup on sloping beaches as well as for studying the interaction between the waves and the coastal structures.

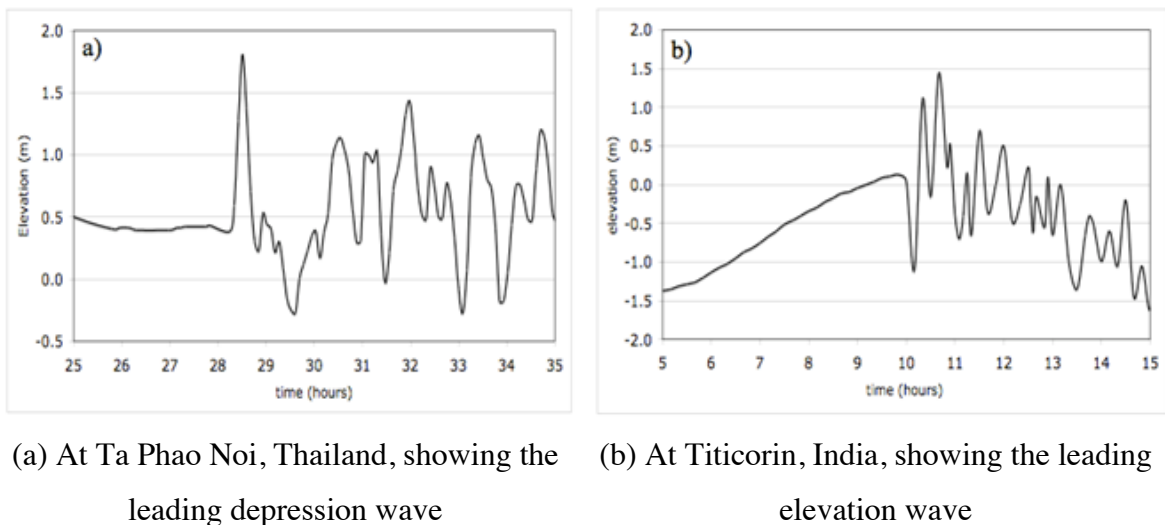
It should be emphasized that solitary waves are not an accurate description for tsunamis in the real world. A typical tsunami generated by tectonic disturbance is so shallow and so linear that the distance necessary for a solitary wave to emerge from the initial source is too long for any ocean on the earth (Hammack and Segur 1978; Yeh et al. 1996; Madsen et al. 2008). Even though real-world tsunamis are not typically in the form of a solitary wave, a solitary wave does possess the characteristics of tsunamis; hence, it is conveniently used as a tsunami model in research.

2.1.1.2 N-waves

Leading waves can be modeled as elevation or depression N-waves. The patterns of the wave are related to the co-seismic seafloor deformation and distance from the seismic fault location. Tsunamis characterized by leading depression N-waves first experience the trough followed by the crest, while leading elevation N-waves experience the crest of the wave followed by the trough. The typical co-seismic displacement occurring at an earthquake event in a subduction zone can be characterized as the formation of land subsidence in the leading zone of the subduction (land side) and ground uplift in the trailing zone of the subsidence (sea side) (Yeh, 2009).

Figure 2-2 shows the difference between a leading depression wave and a leading elevation wave on tide gauge measurements in Thailand and India, respectively, resulting from the 2004 Indian Ocean Tsunami. Note that the source of this event is along the Andaman-Nicobar Islands, subsiding along the east strip and uplifting along the west strip of the co-seismic displacement (see Figure 2-3). Far-source tsunami waves typically

produce leading elevation waves, as observed in India. Locally-generated tsunami waves typically produce leading depression waves, as observed in Thailand. A local tsunami would reach the coastline within tens of minutes after an earthquake, whereas, a distant tsunami, generated by an earthquake far away, will not reach the coast for several hours. The devastating tsunami in Thailand in 2004 was a leading depression N-wave. The same earthquake source produced leading elevation waves farther away in Maldives (Lo & Wang, 2012) as demonstrated in Figure 2-3.



**Figure 2-2: Tide gage records for the 2004 Indian Ocean tsunami (Yeh, 2009)
(Digitized by Robertson, 2007)**

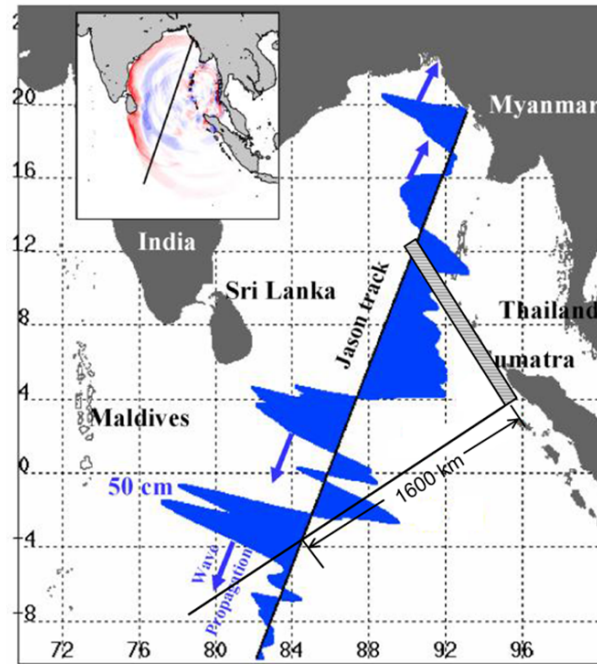
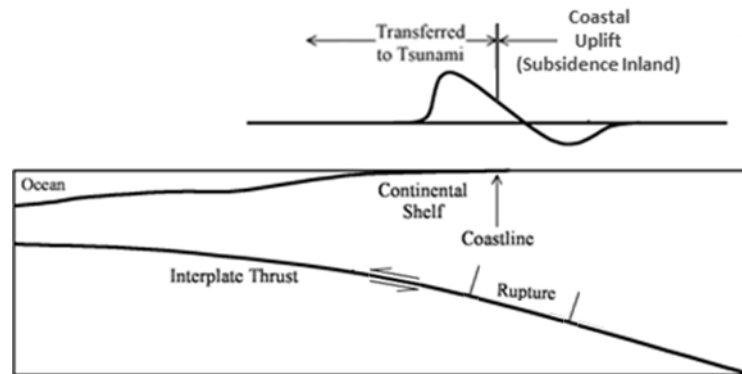


Figure 2-3: Wave propagation of 2004 Indian Ocean Tsunami (NASA, 2005)

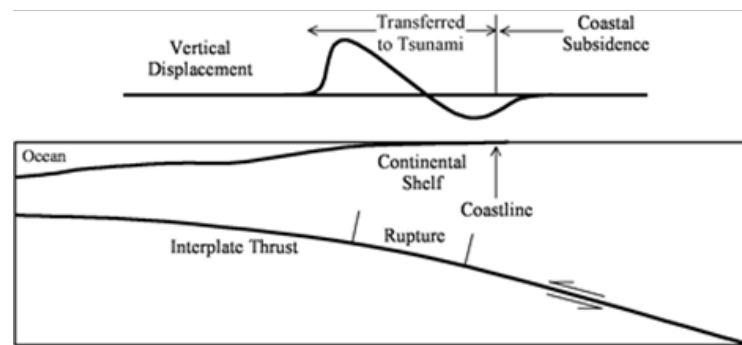
2.1.2 Locally Generated Tsunamis

In locally generated tsunamis, where the rupture of a subduction-type fault occurs near the coast, the displacement of the seafloor and coastline interact and exhibit complex behavior (Geist, 1999). As Figure 2-4 (a) shows, if subsidence due to a fault rupture occurs inland of the coastline then a leading elevation wave will be produced in the direction of subduction (Yeh, 2009). If the subsidence is offshore then a leading depression wave will approach the shore in the direction of subduction, as shown in Figure 2-4 (b) and (c). Furthermore, the subsidence of the coast typically exacerbates inundation (Geist, 1999), making locally generated tsunamis a critical threat due to the short warning time and high inundation potential.

(a) Coastal
subsidence
inland



(b) Rupture
zone adjacent
to coastline
with coastal
subsidence



(c) Deep
water
tsunami

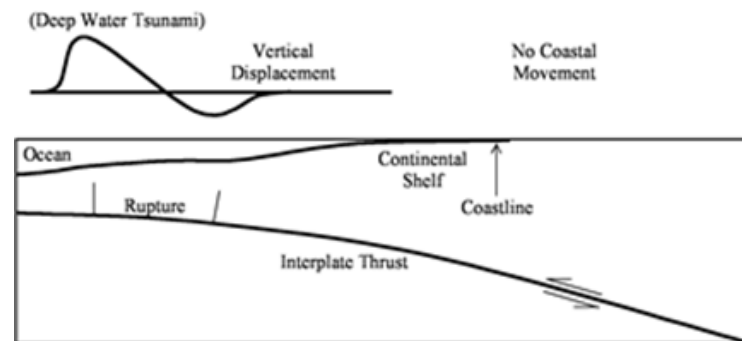


Figure 2-4: Schematic diagrams of the vertical displacement resulting from subduction-type fault dislocation. Source: (Geist, 1999)

Imagine witnessing the shoreline recede back into the ocean followed by a great wave building and crashing onto the shoreline. This occurred in some localities in Japan when a leading depression waveform hit during the 2011 East Japan Tsunami (ASCE-

COPRI-PARI Coastal Structures Field Survey Team, 2013). An earthquake of magnitude Mw 9.0 induced this tsunami approximately 100 km off the coast of Miyagi.

Knowing the expected wave form is important because the waveform influences the tsunami runup characteristics and behaviors. Tadepalli and Synolakis (1996) demonstrated that leading depression N-waves climb higher on a sloping beach than the equivalent leading elevation N-waves. Leading depression waves also typically create a steep wave front and form a breaking wave offshore (Yeh, 2009); after breaking offshore, the wave becomes in the formation of a bore and then to start a surge on to dry land after it reaches the shore.

2.1.3 Far-source Generated Tsunamis

As we discussed earlier, the typical seafloor displacement pattern of the uplift-subsidence combination (see Figure 2-4) suggests that the leading elevation wave would be likely formed when the tsunami propagates towards the ocean (to the left in Figure 2-4). Therefore, far-source-generated tsunamis typically produce waveforms with a leading elevation wave approaching the coastline.

Leading elevation waves often have a gradual increase and decrease of inundation water depth, without violent rushing flows, especially for regions with steep slopes (Yeh, 2009). The 1960 Chile Tsunami observed in Japan is an example of surge flooding from a far-source-generated, leading elevation tsunami wave (FEMA P-646, 2012). The 1964 Alaska tsunami along the coastal communities in Vancouver Island, Canada, is another example of this.

2.1.4 Wavelengths

The wavelength of a tsunami is difficult to define because of its irregular and transient wave motions. Wavelengths can be however inferred by multiplying the wave speed by the wave period. The wave period of the 1960 Chilean Tsunami measured in Japan was approximately 40 to 60 minutes whereas a near-field tsunami is usually 5 to 20 minutes long (Shuto & Fujima, 2009). Based on altimeter-mounted satellites (Jason-1 and

TOPEX/POSEIDON), the 2004 Indian Ocean Tsunami had a wavelength of approximately 500 kilometers (Kulikov, 2006).

2.2 Terrain and Local Conditions

Tsunami heights have been observed to deviate significantly within neighboring areas (Charvet, 2012; International Council for Science Scientific Committee on Oceanic Research Working Group 107, 2002; Shuto & Fujima, 2009). Local terrain can change flow patterns within very short distances (Yeh, 1998). Tsunami effects may be amplified by:

- Wave-wave interactions including resonance in a semi-enclosed bay
- Bathymetry and topography that causes wave-energy concentration, including the wrap-around effects behind an island (Yeh, Liu, Briggs, & Synolakis, 1994).

The National Tsunami Hazard Mitigation Program defines harbor resonance as, “the continued reflection and interference of waves from the edge of a harbor or narrow bay which can cause amplification of the wave heights, and extend the duration of wave activity from a tsunami”.

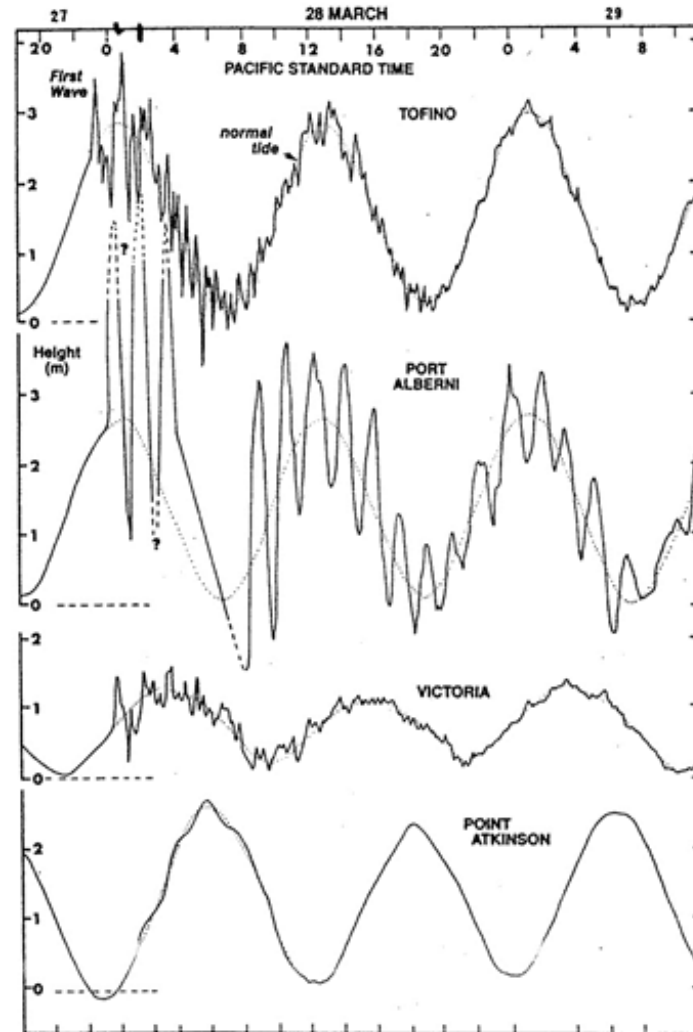


Figure 2-5: Sea level records of tsunami waves at four locations in British Columbia on March 27-29, 1964 (Thomson, 1981; Wigen & White, 1964)

One example of resonance is the 1960 Chilean tsunami. This tsunami produced far-source, long-period waves that resonated in the long Ofunato Bay in the Iwate Prefecture of Japan. Inundation from this wave caused serious damage in areas that had previously been unaffected by near-field tsunamis (Shuto & Fujima, 2009). Due to the complex coincidence of wavelength and local terrain, the tsunami wave effects were underestimated. Another example of resonance is the 1964 Great Alaskan Tsunami, where the tsunami produced a significant amplification within the fjord in Port Alberni,

Canada (Breaker, Norton, Carroll, & Murty, 2009) as shown in Figure 2-5 and Figure 2-6.

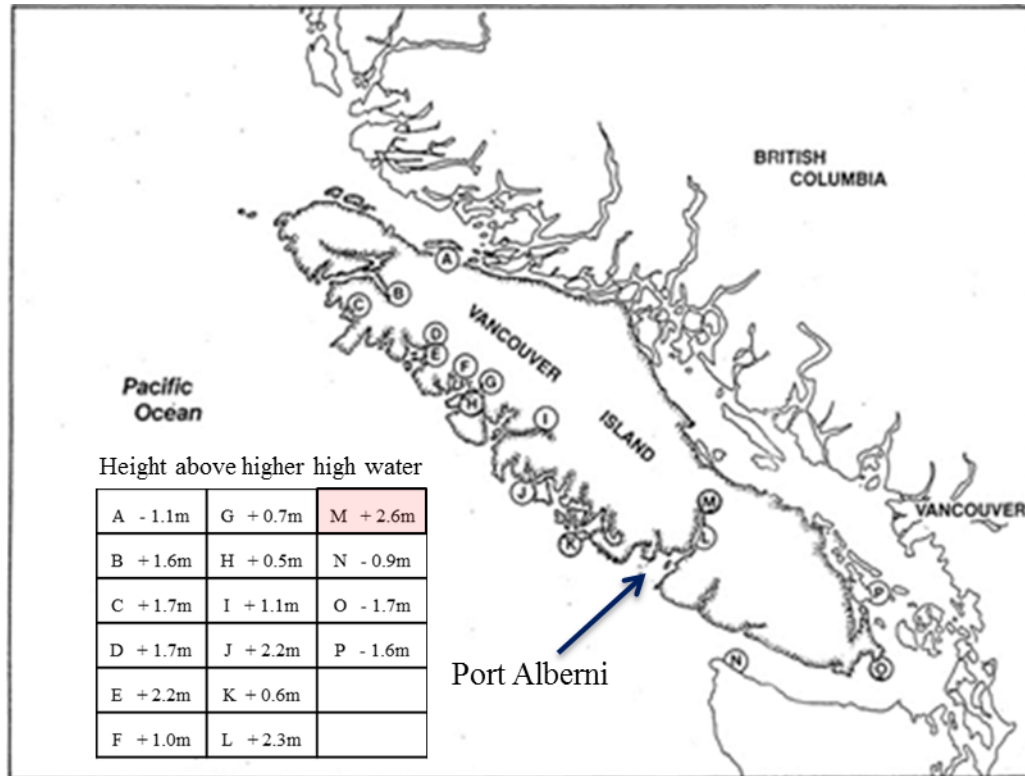


Figure 2-6: Resonance in Port Alberni, Canada (Wigen & White, 1964)

Wave focusing often results at the head of V-shaped bays (e.g. the ria-type coastal lines). This mechanism caused significant tsunami runup amplification along the Sanriku Coast, Japan, during the 2011 East Japan Tsunami event. Steep slopes and narrow valleys in a region near the shoreline are capable of causing amplification. For example, during the 1993 Hokkaido Nansei-Oki Earthquake Tsunami, the highest runup (32 m) was observed at the end of a narrow valley on the west coast of Okushiri Island, Japan (Shuto & Fujima, 2009).

For regions like the valley on Okushiri Island, little energy attenuation occurred because the wave traveled a relatively shorter distance of the inundation than for regions without slopes. On the other hand, substantial energy would be lost by friction in the process of tsunami runup on a beach with very mild slope (e.g. flat coastal plain).



(a) Strong buildings with very few gaps for flow



(b) No gaps between housing

Figure 2-7: Channeling Effects in Callao, Peru (Photo courtesy of Harry Yeh)

Land development in the area can also significantly contribute to flow conditions. Buildings not immediately washed away during a tsunami can provide shielding effects, reducing wave forces, or channeling effects, amplifying wave forces, on the surrounding structures. One potential problem where the channeling of water may occur due to land development is in the streets of Callao, Peru. No gaps exist between structures, as shown in Figure 2-7, which may create flow focusing and channeling effects.

2.3 Bathymetry

Just as local terrain affects tsunami waves, the bathymetry leading up to the shoreline plays a major role in defining tsunami wave characteristics. The problem is that obtaining detailed bathymetric details is costly and must have high resolution in order to produce accurate results (Titov & Synolakis, 1998); (Titov et al., 2005); (Mader, 2004). An amplification factor correcting for the lack of detailed bathymetry data has been suggested by correlating observed runup heights with computed tsunami amplitudes on various coasts, however, it has only been calibrated for constant slopes (Rossetto, Allsop, Charvet, & Robinson, 2011).

2.4 Laboratory Testing

In an attempt to accurately predict tsunami forces on buildings, researchers try to conduct simple experiments correlating parameters of depth and velocity to forces. The experiments typically generate waves using a dam-break (Cross, 1967; Keulegan, 1950; Ramsden, 1993), piston-type paddle (Asakura et al., 2002; Fujima, Achmad, Shigihara, & Mizutani, 2009; Santo & Robertson, 2010), or pneumatic wave generator (Charvet, 2012; Togashi, 1986).

Tsunamis' very long wave length is one of the factors that make scaled-down laboratory simulations for tsunamis extremely challenging. The Froude scaling is used to scale tsunamis from a real ocean to a laboratory environment. Consider the 500 kilometer wavelength of the Indian Ocean tsunami at a depth of 4000 meters offshore, for example. If a laboratory experiment has a 0.5 meter deep basin that is quite deep for the laboratory scale, the wavelength will still need to be 62.5 meters long, which is extremely difficult to generate in existing laboratory facilities: for a reasonable laboratory simulation with 5 ~ 6 wavelengths, a wave basin with 350 m long or larger would be necessary. Test basins also need to be deep enough so viscous effects are weak over most of the wave evolution.

For simulating near-shore tsunamis in the laboratory, an experiment might simulate a tsunami wave in 200 meter deep water with a wavelength of 10 kilometers in a tank with water 0.5 meters deep; even this set-up would require a wavelength of 25 meters. Such a long wavelength is extremely difficult to be generated in the laboratory.

3 TSUNAMI STRUCTURAL ANALYSIS

The goal of this section is to discuss current approaches used to determine tsunami forces on a building and describe possible approaches to determine the global and local forces needed to design the structures. Most tsunami wave force formulations depend on water wave height and velocity parameters, which are difficult to estimate without numerical modeling and often are not described with consistent terminology. Therefore, input parameters required for force estimation will be considered on two levels: (a) when maximum inundation depth or runup elevation is the only parameter available; or (b) when numerical analysis provides specific height and velocity terms.

This chapter presents a description of building global failures (overturning and sliding) observed in the aftermath of tsunami events, such as the Japan 2011 event, as well as a description and discussion of the important definitions used for the tsunami intensity measures (velocity and height/depth) that affect the form and values that should be considered in tsunami force estimation. Once the main intensity measures are described, the various tsunami forces are described and close attention is given to the definition of the physical aspects and phenomena that characterize the different forces. Among these physical parameters that affect the forces, an emphasis is given to building shapes since it is an important parameter that affects greatly the forces that can be developed and expected. There is a lack of information for irregular building shapes, such as U-shaped buildings.

3.1 Observed Failure Modes

The Building Technology Research group in Japan specifically discusses three failure modes: rotation, sliding, and collapse (Fukuyama et al., 2013). Rotation being defined as the global overturning of a building, sliding defined as the global translation of a building, and collapse being the failure of one or more individual structural components. To have a complete analysis of these failure modes, consideration must be given to soil stability and scour as they are critical components of the analysis (Yeh & Mason, 2014); however, due to the complexity of the subject, scour will not be discussed in detail within the scope of this thesis.

3.1.1 Overturning

The recent East Japan Tsunami in 2011 revealed that many engineered buildings failed due to overturning (Yeh et al., 2013). Only a few papers from the Building Research Institute in Japan have begun to discuss this failure mechanism (Okada et al., 2006). The March 11, 2011 East Japan Earthquake and Tsunami witnessed many failures in reinforced concrete buildings due to rotation. These failures were attributed to higher than expected inundation depths, high velocities, soil scour, and buoyancy effects (Yeh et al., 2013). As shown in Figure 3-1, the velocity and height do not have maximum values at the same point in time. Therefore, FEMA P-646 (2012), adopted the use of a term called the maximum momentum flux $(hu^2)_{max}$, to capture the input values that would produce the greatest force on a building. Following the same logic for the overturning moment, the product $h(hu^2)_{max}$ would be an inaccurate representation of the moment without re-determining the maximum value for $(h^2u^2)_{max}$, which is the term proportional to the overturning moment. The maximization of these parameters is necessary to avoid using the maximum values concurrently when they occur sequentially, i.e. using h_{max} and u^2_{max} concurrently, when they occur at different time intervals. The maximum quantity of the term $(hu^2)_{max}$ is based on a time history analysis. It is over-conservative to use maximum depth and maximum velocity simultaneously, when they occur at different instances in time. Inversely, it may not be conservative to use equations for momentum flux with the associated inundation depth to determine the moment exerted on a building, since the momentum flux was optimized to provide the maximum value proportional to (hu^2) not (h^2u^2) . The moment is a function of (h^2u^2) and therefore the maximum moment may occur at a different time than the maximum momentum flux.

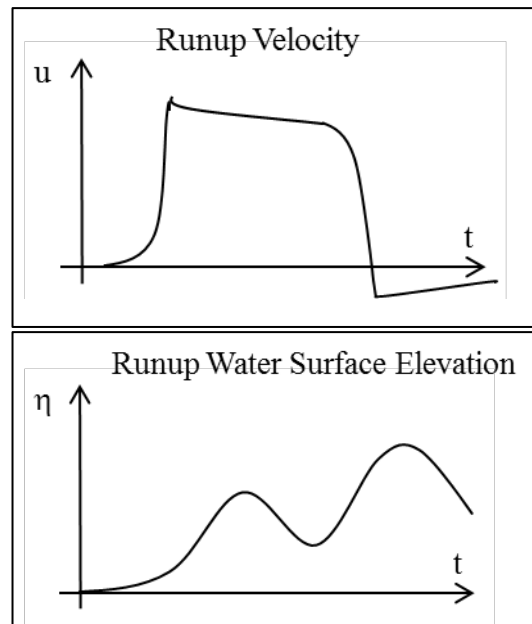


Figure 3-1: Height & Velocity Relationship Sketch (Source: Asakura, 2002)

The rate of water level increase is also important. For example, the overturned buildings in Oganawa, Japan were not hit with large impulsive forces due to the increase in water depth (~20 meters), however, the hydrodynamic and perhaps buoyancy forces are responsible for the overturning failures in Onagawa.

Buoyancy effects and foundation scour are very important factors in the evaluation of rotation failures. The reduction of the weight of a structure by buoyancy promotes overturning, and the soil acts as a resistance force against overturning. The greater the buoyant force and the more scour, the more susceptible a building is to overturning failure.

In summary, to date (h^2u^2) is a term that has not been provided previously, but it is needed to compute the peak overturning moments.

3.1.2 Sliding

Sliding is a concern when lateral forces are large. Buoyancy decreases the bearing of the structure on the soil and reduces the ability of friction to resist sliding forces. Another important factor to consider is the realistic maximization of velocity and depth.

3.2 Definition of “Flow Velocity”

The terms used for “flow velocity” have unique physical meanings and applications, which cannot be transposed. This section will discuss the different velocities associated with tsunami-effect evaluations. Not all of the terms below are correlated to force parameters; however, they should be distinguished in the following way:

- a. Velocity of surge
 1. Velocity of surge front: the leading edge of a tsunami surge advancing onto a dry ground surface. This velocity is based on the prediction of frictionless (inviscid) runup motion where the depth at the leading edge is nil.
 2. Velocity of fluid in surge head, u_0 . This is the velocity of the real leading head formation influenced by viscosity, where the depth at leading head is finite.
- b. Velocity of bore front, c . This is the speed of bore advancing onto another flow in front of it. This is not the fluid-material velocity and is frequently assumed to travel over still-water.
- c. Velocity of fluid behind bore front, u .
- d. Velocity of fluid at maximum value of the linear momentum flux, hu^2 ; note that this is not the maximum fluid velocity.
- e. Velocity of fluid at maximum value of h^2u^2 , the parameter that is proportional to the maximum moment at the base of a structure.
- f. Maximum velocity of debris carrying fluid; note that debris can be carried only when the water depth is above the minimum threshold of debris draft.

3.3 Definition of “Flow Depth”

Depths associated with a dam-break surge and/or a bore are labeled in Figure 3-6 and Figure 3-7 respectively and described as follows:

- a. Depth of the surge head, h . This is the water depth immediately behind the tsunami front, running up the dry surface. This depth results from the formation of the ‘tip’ boundary layer and is identified by Whitman (1955) and Kuelegan (1950)

- b. Water depth in front of the advancing bore, h_s
- c. Flow depth behind the bore front (quiescent and bore combined), h_b
- d. Height of a bore, $h_j = h_b - h_s$
- e. Depth of the reservoir in a dam break scenario, H
- f. Depths ill-defined, h
- g. Maximum inundation depth at the site of interest, η_{\max}
- h. Flow depth at the maximum value of the linear momentum flux, hu^2
- i. Flow depth at maximum value of h^2u^2 , the parameter that is proportional to the maximum moment at the base of a structure
- j. Flow depth of debris carrying fluid; note that debris can be carried only when the water depth is above the minimum threshold of debris draft

As discussed earlier, the term “height” is typically in reference to some elevation above the tide level at the event of a tsunami as a datum; however, it is also used to describe portions of flow, such as the height of the bore, where the entire water depth is segmented. The term η can be distinguished from as representing a height determined by a numerical model.

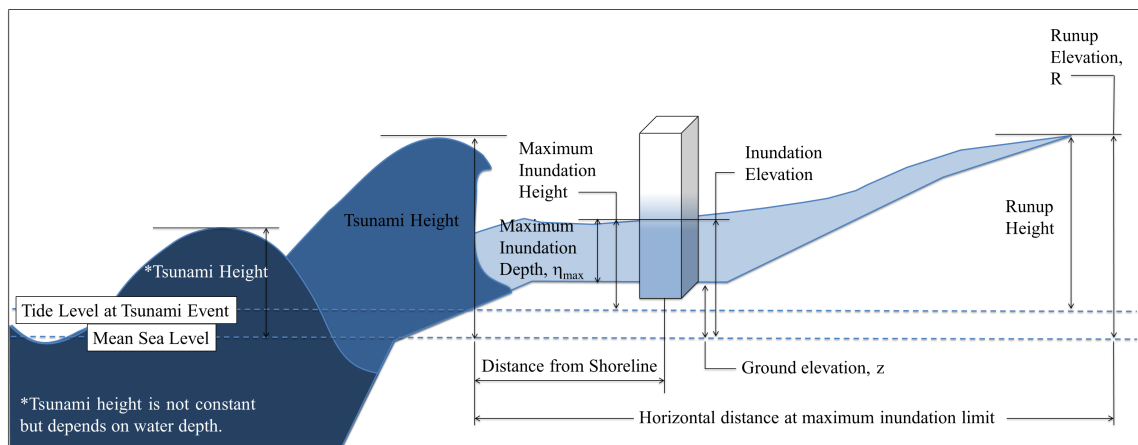


Figure 3-2: Tsunami Design Terminology
Adapted from: (Chock, 2012)

The elevation above mean sea-level of the furthest location of inundation is denoted by the variable, R^* ; the ground elevation of the location of interest is denoted by

the variable z as shown in Figure 3-2 and Figure 3-3; the height above ground level of a specific location on a building is denoted by the variable, y .

As previously mentioned, the runup can be described as the maximum height of water onshore above the tide at the time of the tsunami (National Tsunami Hazard Mitigation Program, 2005) or as the height at the furthest point of inundation (FEMA P-646, 2012). This should be specified by the source of the runup data. FEMA P-646 recommends an estimate of inundation based on the parameters of the runup elevation, R^* , and the ground elevation, z , of the structure being designed as shown in Eq 1 and Figure 3-3.

$$h = 1.3 R^* - z \quad \text{Eq 1}$$

When only R^* and z values are available, FEMA P-646 has adopted equations to estimate velocity and momentum flux parameters. This error in the formulas based on R^* and z is documented by FEMA P-646 (2012). A situation like the one displayed in Figure 3-3 is likely to occur where there is steep coastal topography, such as the coastal cliffs in Tohoku, Japan (FEMA P-646, 2012).

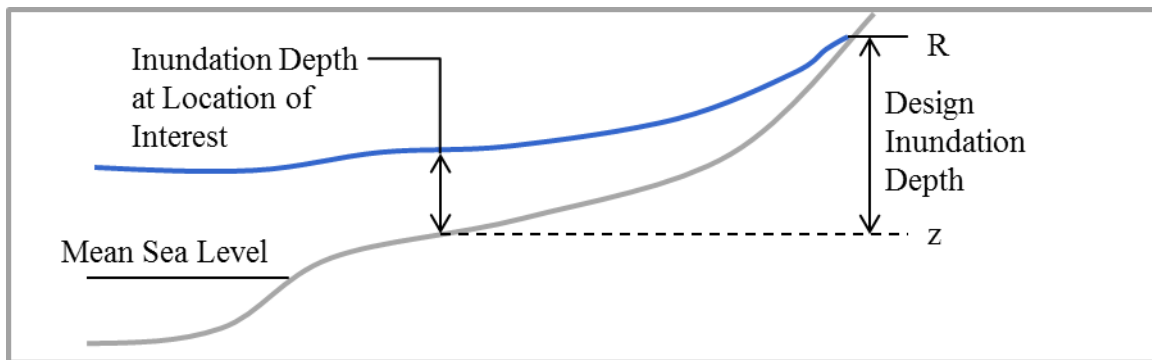


Figure 3-3: Over-conservative Inundation (Adapted from FEMA P-646, 2012)

On the other hand, locations with relatively gradual and flat topography, where the runup basin scale is smaller than the tsunami, like in Onagawa, Japan, are likely to have inundation similar to the one depicted in Figure 3-4 (FEMA P-646, 2012). In this

case, the difference between R and z gives the most accurate description of inundation depth. Many examples of flat coastal plains can be found in the western United States, such as the Long Beach Peninsula, Washington; Tillamook, Oregon; and many coastal plains in Southern California.

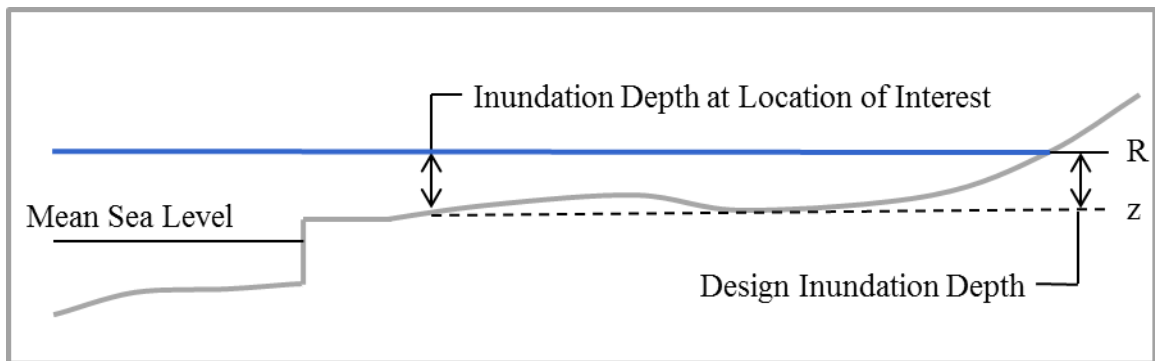


Figure 3-4: Well-predicted Inundation (Adapted from FEMA P-646, 2012)

A dune followed by flat and wide topography, such as the Sendai Plains in Japan may have maximum runup heights at the beach berm near the shore and have much smaller runup elevations, R , as shown in Figure 3-5. This could be a dangerous under-prediction of forces if using Eq 1 to obtain design forces since the true inundation depth would be under-predicted by the difference between the runup height and the site elevation.

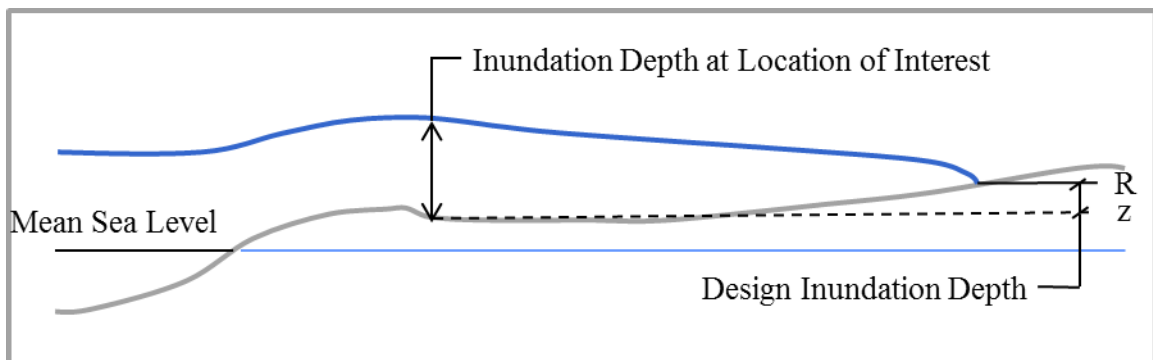


Figure 3-5: Under-predicted Inundation (Adapted from FEMA P-646, 2012)

3.4 Surge Front vs. Bore Front

Due to the reduction of the water depth and the very long wavelength of the tsunami, a tsunami often breaks offshore (from the shoaling effect) forming a bore. A bore can be described as a broken wave having a “steep, violently foaming and turbulent wave front, propagating over still water of a finite depth”(FEMA P-646, 2012). A surge can be defined as the tsunami bore once it reaches land and is continuing to rush over dry land (FEMA P-646, 2012).

3.4.1 Surge

Keulegan (1950) conducted an experiment using a dam-break scenario over dry land. This is a dry-land “surge”. The bore front is considered as a solid body. He defined the velocity as shown in Eq 2. This is the velocity described in Figure 3-6.

$$u_0 = 2\sqrt{gh} \quad \text{Eq 2}$$

In this experimental set-up, h is not well defined as shown below in Figure 3-6. It is described as the point at which viscosity (friction) takes effect; however, the precise location is difficult to measure.

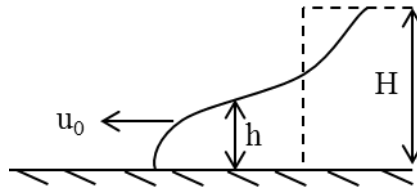


Figure 3-6: Surge Definition Sketch (Keulegan, 1950)

Cross (1967) also conducted dam-break experiments that included, first, a dry-bed and second a bore propagating on standing water. Cross referenced an equation developed by Fukui, Nakamura, Shiraishi, and Sasaki (1963) for the velocity of a bore on dry-bed. In this equation, the velocity of the surge front was defined based on a Manning coefficient of 0.013 and an experimentally determined roughness coefficient, and was expressed as shown in Eq 3.

$$u_0 = 1.83\sqrt{gh} \quad \text{Eq 3}$$

Based on his experiments, Cross (1967) concluded that bores on standing water showed steeper wave front slopes than surges on dry land. Many years later, this finding was verified by Ramsden (1996). However, bore velocities on standing water are approximately 85% of the corresponding surge velocity on dry-land (Cross, 1967; Keulegan, 1950). Similar to Figure 3-6, the h in this equation is not well defined.

FEMA P-646 uses velocity based runup theory for inviscid fluids developed by Yeh (2007). The equation used in FEMA P-646 (2012) for surge velocity is:

$$u_0 = \sqrt{2gR \left(1 - \frac{z}{R}\right)} \quad \text{Eq 4}$$

where, u is the maximum velocity of the leading edge of a runup surge front and it is considered a solid body. FEMA P-646 adapts this equation by multiplying a safety factor of 1.3 to the runup elevation, “ R^* ”, as shown in Eq 5.

$$R = 1.3 R^* \quad \text{Eq 5}$$

3.4.2 Bore

The velocity of a bore front, represented by c in Figure 3-7 (a), can be described using an analogy of a hydraulic jump as shown in Figure 3-7 below. The different heights are distinguished with subscripts: h_j represents the height of the “jump” or the height of the bore above what was previously still-water, h_s represents the height of the still-water, h_b represents the total height of the bore from the ground to the water surface, c represents the bore propagation speed, and u represents the combined material velocity.

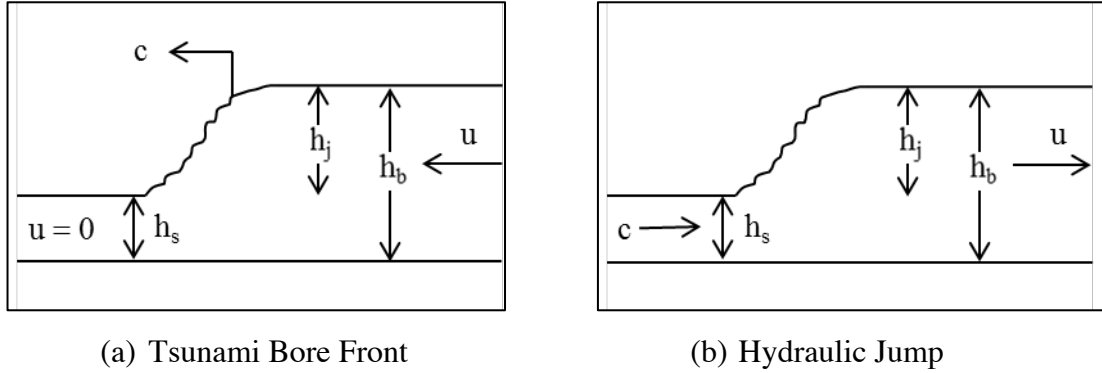


Figure 3-7: Hydraulic Jump - Bore Front Analogy (Mohamed, 2008)

The hydraulic jump equation is identical to the bore equation by moving the coordinates with the bore propagation speed, c . By assuming a moving frame of reference with an incoming bore, the equation for the speed of bore propagation is given by:

$$c = \sqrt{\frac{1}{2}gh_s \left(1 + \frac{h_b}{h_s}\right)} \quad \text{Eq 6}$$

where g is the acceleration due to gravity, and the height parameters as defined in Figure 3-7. Note that this equation is for the velocity of a bore front, not the fluid material velocity. The fluid material velocity, shown as u in (a) of Figure 3-7 is more appropriate for force calculations such as the hydrodynamic force. Even so, these parameters are unlikely to be available when designing for a structure on the coast. The equation for u for a bore propagating over still water is given below:

$$u = c \frac{h_j}{h_j + h_s} = c \frac{h_j}{h_b} \quad \text{Eq 7}$$

3.5 Forces

Force determination has been differentiated in some guidelines depending on whether the flow is acting on a wall component or a structural element. It is worth noting,

however, that fundamentally, fluid forces exerted on a body (e.g. building) – which are a vectorial quantity – are given by:

$$\vec{F} = \int_{\partial S} \tau_{ij} n_j ds \quad Eq\ 8$$

where τ_{ij} is the stress tensor, n_j is the unit vector pointing perpendicularly outward from the surface ds , and ∂S is the surface of interest. The integrand can be categorized by two components, namely, the one normal to the surface ($i = j$) called pressure force, and the vector component tangent to the surface that is called shear force. These are the origin of the tsunami forces described next.

3.5.1 Hydrodynamic Force

The hydrodynamic force is characterized by steady flow past an object fully enveloped in water. The force is primarily affected by the shape and size of the object, which is adjusted by a coefficient of drag/resistance. The drag is a component of the total force parallel to the ambient velocity, and the perpendicular component is called the lift force. When the body is fully submerged in a steady flow, then the drag force is given by:

$$F_D = \frac{1}{2} C_D A \rho u^2 \quad Eq\ 9$$

where C_D is the drag coefficient, A is the projected area of the body on a plane normal to the direction of ambient steady velocity that has magnitude u , and ρ is the fluid density (including sediments). Note that part of the drag force is due to *skin friction* (i.e. tangential viscous shear stress force along the body) and part is due to the pressure distribution around the body, called *form drag*. It is evident that the hydrodynamic force is caused by a relatively steady motion between the fluid and the individual submerged body itself. The integration surface ∂S of the general force Eq 8 represents the complete surface identifying the entire body.

Eq 9 is often used for a semi-submerged body. Arnason, Petroff and Yeh (2009) recognized, however, that the traditional use of Eq 9 is for a fully submerged body under steady-state conditions; therefore, instead of the drag coefficient C_D , the terminology “coefficient of resistance” C_R was introduced to distinguish the forces on a surface piercing cylinder under quasi-steady flow conditions, as shown in Figure 3-8. Thus, the hydrodynamic force is also known as the resistance force (Arnason et al., 2009).

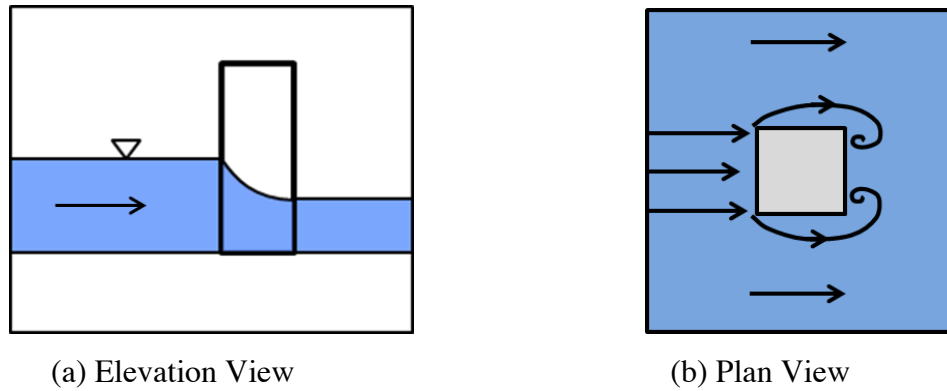


Figure 3-8: Hydrodynamic Force Assumption

Arnason et al. (2009) found that the magnitude of the coefficient of resistance C_R is comparable (approximately 2.0) to C_D for a square column. It is anticipated that for a not-too-elongated body in the flow direction, the dominant force is due to form drag, which is caused by the pressure difference (roughly equivalent to the water-surface difference in front and back of the body). Evidently, the use of Eq 9 to estimate force on a portion of the body (e.g. windows, walls etc.) does not make sense. In summary, the equation form from Eq 9 that is often called the hydrodynamic force must be used to evaluate fluid force on a body as a whole when subject to steady (or quasi-steady) flows.

FEMA P-646 provides an equation for the hydrodynamic force, which is given as:

$$F_D = \frac{1}{2} C_D \rho B (hu^2)_{max} \quad \text{Eq 10}$$

where C_D represents the coefficient of drag (typically 2.0), ρ is the density of water, including sediments, B is the base width of the structure and $(hu^2)_{max}$ is the maximum moment flux (FEMA P-646, 2012). Depending on tsunami characteristics and the shape of the tsunami evacuation building, and its dimensions, the tsunami wave may not fully envelop the structure, for example, seawalls.

3.5.2 Hydrostatic

The hydrostatic force is due to a fluid condition in which the pressure force balances with the gravitational body force:

$$\frac{\partial p}{\partial z} = -\rho g \quad \text{Eq 11}$$

where p is the pressure and g is the gravitational acceleration. The hydrostatic condition is realized when the inertial force is absent. The hydrostatic force can be calculated by integrating the pressure field obtained in Eq 8 over the surface of interest. Because the pressure is independent of the horizontal direction, there is no net hydrostatic force *if* the integration can be made around the entire body submerged in the constant water level (note that the integration of the vertical component produces a net upward force, call buoyant force). Under the hydrostatic condition surrounding a body, the net horizontal force is nil. However, the hydrostatic force can be used to calculate the force acting on one side of a contained liquid or on the side of a component surface (e.g. columns, walls and windows). Under the condition of fluid in motion, the force computation should no longer be considered as hydrostatic around the body due to the induced vertical acceleration (inertial force per unit mass) associated with the formations of wake in the leeward side of the building shape and the generation of horseshoe vortices in the front face of the building being subjected to the flow conditions. It must be emphasized that the force acting on the body in the flow is still pressure force, but it is not hydrostatic. Nonetheless, when the vertical flow acceleration at the body is weak – which may occur in a very gradual tsunami inundation process – the tsunami forces acting on the surface of

the body (e.g. windows, column, walls) can be approximated under the hydrostatic condition based on the water surface on the body surface.

The hydrostatic force is a function of the height of inundation and the density of the water surrounding the building. The pressure distribution is in the shape of a triangle, linearly increasing with depth. As illustrated in Figure 3-9, there are three main scenarios for considering the hydrostatic case on the structure at the global scale:

- a.) Gross Hydrostatic: The maximum inundation is present only on one side of the wall
- b.) Hydrodynamic: A discrepancy exists between water level at the front face of the building and back face of the building. This case is more appropriately evaluated by Eq 9, i.e. the hydrodynamic force.
- c.) Zero Net-hydrostatic Force: Individual components still have pressure force exerted on them, especially if the building is airtight, however, no global force is exerted on the building to produce sliding or overturning.

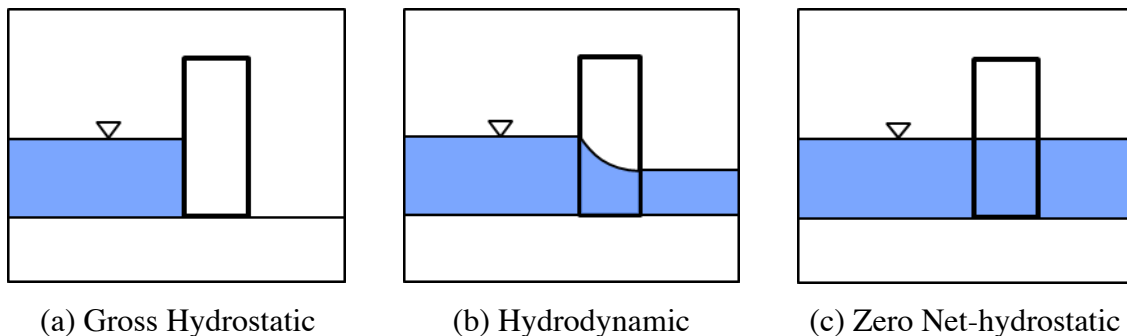


Figure 3-9: Stages of Hydrostatic Force Application on a Global Scale

The hydrostatic force is not a major concern for the global failure mechanisms of sliding or rotation once water fully envelopes the structure, as shown in of Figure 3-9a. In such a case, the building is most susceptible to the failure of individual structural elements, such as columns or walls. Otherwise, only local structural components need to resist the hydrostatic pressure if no fluid enters the building. As it turns out, the hydrostatic force can act as a stability force on the back-face of a building, where the net

force is pushing back against the oncoming wave forces. However, the extreme lateral forces may be underestimated in cases where the back side of a building is not fully inundated. Most force combinations neglect to consider this intermediate stage after the impulsive force acts on the building but before the water fully envelopes the structure and induces a hydrodynamic force on the structure. These last considerations are currently not included in the FEMA P-646 guidelines, and the author of this thesis is not aware if such considerations are taken into account in the future ASCE 7 document (Chock, 2012b).

3.5.3 Buoyant Force

The buoyant force is the net upward pressure force acting on a partially or totally submerged body. This vertical force is computed by Eq 8 based on the hydrostatic field given by Eq 11. The buoyant force is equivalent to the fluid weight displaced by the body. It is calculated using Archimedes' principle of volume displacement. An upward force is created equal to the volume of air and other materials occupied by the portion of the building underwater. This is especially important for water-tight buildings, where a much larger volume of air has displaced water. For buildings with breakaway windows/walls, the air trapped above openings (yet below the water line) still needs to be accounted for as a contribution to the buoyancy force. Upward buoyant forces reduce the net weight of the structure, making it more susceptible to both sliding and overturning failure.

The key to understanding this force correctly is to recognize that the origin of the force is the pressure force exerted on the bottom surface of the body (e.g. building). Consider a building with basement that is inundated by a tsunami. To establish the upward pressure force under the building, pore-water pressure in the soil must be increased by the excess water weight on the ground surface by inundation; the pore-water pressure is the one that transmits the loading laterally and underneath the building. It is noted that the pore-water pressure field is governed by the diffusion process that takes a finite time to establish the pressure increase. Based on this behavior, it is conjectured that the effect of buoyant force must depend on: (1) duration and depth of tsunami inundation,

and (2) the depth of bottom surface of the body (building). In other words, in terms of the tsunami's buoyancy effect, buildings with a basement should be more resilient than those without a basement. In fact, it was observed that most of the RC buildings that failed in the town of Onagawa, Japan did not have basements.

3.5.4 Impulsive Force

The impulsive force is defined as the “sudden slam of a steep front of a bore” (Yeh, 2007), and the magnitude of the impulsive force is a factor of both wave steepness and water velocity. At initial water impact, the impulsive force should be less than the subsequent hydrodynamic force if produced by a surge (i.e. propagation on a dry bed). Thus, as it is defined in Yeh (2007), the impulsive force is typically associated with bores propagating in a finite depth of water, since dry-bed surges exhibit a relatively mild slope of the wave front (FEMA P-646, 2012).

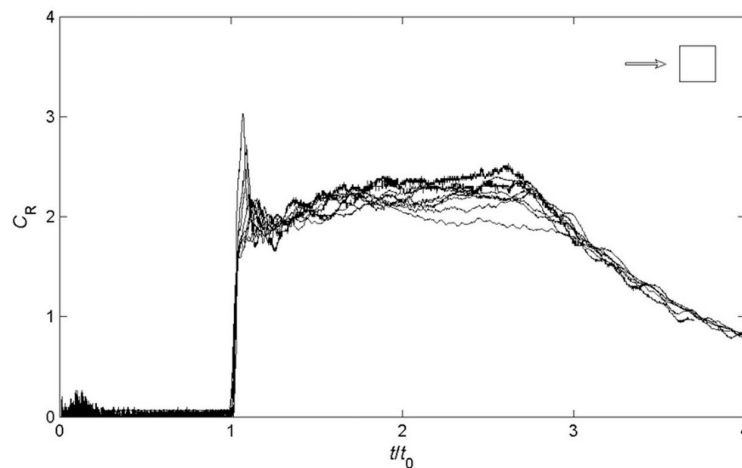


Figure 3-10: Empirical Relationship of Impulsive Force to the Hydrodynamic Force (Arnason et al., 2009)

The impulsive force of the bore has been empirically determined as 1.5 times the hydrodynamic force as shown below in Eq 12 (Árnason, 2005; FEMA P-646, 2012; Ramsden, 1993; Yeh, 2007). A time plot of total force over time is shown in Figure 3-10; both axis' have been nondimensionalized thus representing the coefficient of resistance

and a relative time scale. Though determined through experimentation, the relationship between a transient force (impulsive) and a quasi-steady-state force (hydrodynamic) should be re-evaluated due to the difference in force types, since the formula for impulse is based on a steady-state environment, although it is describing a force that occurs in a very transient stage.

$$F_s = 1.5F_D \quad \text{Eq 12}$$

It is also important to note that the impulsive force hits the leading edge of the most closed-off part of a building and is followed by the hydrodynamic force; the two forces will not occur simultaneously for the same wave.

Paczkowski et al. (2011) determined the force exerted on a wall due to the impulsive force of a bore, as shown in Eq 13 below. The formula includes a number of terms which would be difficult to incorporate in design including the velocity of the bore, u_j ; the height of the bore, h_j ; which does not include the still water depth, h_s . The total height of the bore and still-water is described by h_b . This formula is based on the assumption of still-water prior to the arrival of the bore as well as a Froude number, F_r , of 1.0 of the reverse velocity (the wave bouncing off the wall). It is interesting to note that typical parameters used for the Froude number are 2 for smooth surfaces and 0.7 for rough surfaces (Okada et al., 2006), FEMA-P-646 uses a Froude number of 1.41 (2012). Values of the Froude number for surges are typically 1.83 (Cross, 1967), or 2 (Keulegan, 1950). Mohamed (2008) gives a table of Froude numbers obtained from experiments ranging from 1.14 to 3.13, although these Froude values are not comparable since the equation proposed by Paczkowski assumes the Froude number for a different height, specifically for the height of the return flow.

$$F = \frac{1}{2}\rho gh_b^2 + \rho h_j u_j^2 + \rho g^{\frac{1}{3}}(h_j u_j)^{\frac{4}{3}} \quad \text{Eq 13}$$

Paczkowski compared his experimental vis-à-vis results obtained using Eq 13 to the ones obtained using formulas from Cross (1967), Asakura (2002), and Fujima

(2009b). This comparison seems to have used inconsistent definitions for the depth, which is thought to explain bias in Asakura's results as presented by Paczkowski. The definition used to derive the predicted Asakura data points was based on a "maximum inundation depth" only including the bore height, h_j . This may be a reason for the underestimation of forces based on Asakura's formula. It seems the assumptions with respect to the Froude number and velocity of the still water were selected to fit the data to the predicted vs. experimental curve. Additionally, Asakura's and Fujima's equations were based on experiments with flow surrounding a test structure, while the data from Paczkowski (2011) corresponds to forces exerted on a wall.

3.5.5 Debris Impact

The impact of debris is a significant contribution to the maximum force sustained by a building during a tsunami, depending if there are a large number of debris sources in the local area. Figure 3-13 shows a scenario of debris hitting a building. Sources of debris can vary from place to place but primarily will include automobiles, shipping containers, driftwood, material from wood-frame construction, adobe buildings, and possibly debris from bridges. A number of models for estimating debris have been established as described below.

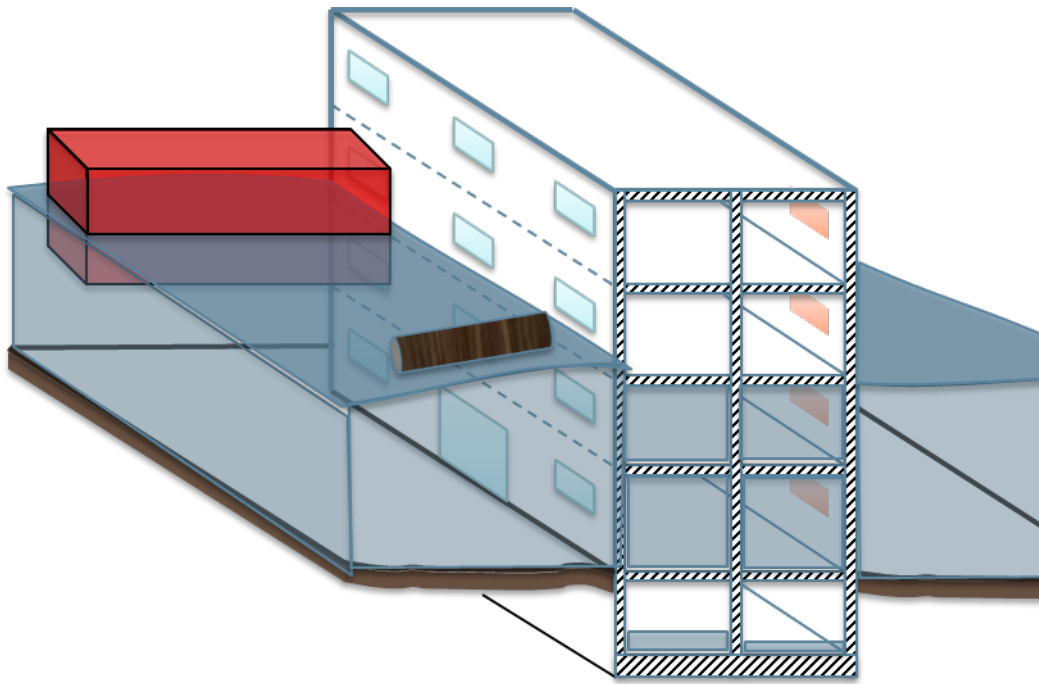


Figure 3-11: Debris Impact Force (Courtesy of Andre R. Barbosa)

Haehnel and Daly (2002a) describe three prominent methods of estimating the force from debris impact, each with significant assumptions. These are the: (i) impulse-momentum approach, (ii) work-energy approach, and (iii) the constant stiffness approach. The experiments by Haehnel and Daly were designed to evaluate the impact of woody debris in a riverine environment. The methods require input parameters that are difficult to estimate: stopping time, stopping distance or a constant stiffness parameter. Below, a description of each of the methods is performed, but it is worth noting that the constant stiffness approach is the easiest to use for specific types of debris. However, the reported stiffness coefficients are limited to the sources of debris that have been previously studied, which include sources from woody debris (Haehnel & Daly, 2002a), rectangular steel tubes (Paczkowski et al., 2011), and shipping containers (Peterson & Naito, 2012). Furthermore, the orientation of the debris and the ability of the debris to deform drastically affect the force produced by the debris (Haehnel and Daly, 2002), which limits the reliability of the constant stiffness approach. Another point discussed is the “added mass coefficient.”

3.5.5.1 Impulse-Momentum Approach

The Impulse-Momentum approach is based on the definition of impulse, as shown in Eq 14 below:

$$I = \int F(t)dt \quad \text{Eq 14}$$

where $F(t)$ is the debris force acting on the structure as a function of time, assumed to be a sinusoidal function. It is assumed that the momentum changes to zero within a certain period of time. The integrated force is described by the change in momentum as $F = \frac{m u}{\Delta t}$ where m is the mass of the debris, u is the initial velocity of the debris, and Δt represents the impact time from initial contact of the debris with the structure to stopping time. This method requires an estimate of impact time and velocity at the time of impact. If the force function $F(t)$ is assumed to be sinusoidal, the maximum force can be determined by multiplying the average force $\frac{m u}{\Delta t}$ by $\frac{\pi}{2}$ to obtain the maximum force as shown in Eq 15 below.

$$F = \frac{\pi u m}{2 \Delta t} \quad \text{Eq 15}$$

3.5.5.2 Work-Energy Approach

The Work-Energy approach is based on the principle of work, where work is equal to the integral of force over stopping distance Δx and equal to kinetic energy KE , shown in Eq 16:

$$W = \int F(x)dx = KE = \frac{1}{2}mu^2 \quad \text{Eq 16}$$

Substituting the product of the spring constant, k , multiplied by the displacement, x , for the force, F , the equation is now $W = \int kx dx = KE = \frac{1}{2}mu^2$. Taking the integral

of the left-hand side of the equation, $W = \frac{1}{2} k x^2 = KE = \frac{1}{2} m u^2$, then re-substituting $\frac{F}{x}$ for the assumed constant k , the net result is $W = \frac{1}{2} F x = KE = \frac{1}{2} m u^2$. This last equation can be rearranged to produce the term for force as shown in Eq 16.

$$F = \frac{m u^2}{\Delta x} \quad \text{Eq 17}$$

It is worth noting, that this approach requires the stopping distance of the debris, Δx , which is difficult to predict and standardize.

3.5.5.3 Constant-Stiffness Approach

The constant-stiffness approach derives the force assuming a spring system using the dynamic equation, shown in Eq 18:

$$m\ddot{x} + k_e x = 0 \quad \text{Eq 18}$$

where m represents the mass of the debris, \ddot{x} represents the second derivative of the distance traveled in the positive x direction from rest with respect to time t , and k_e represents the effective contact stiffness of the spring with units of force per distance displaced, as shown in Figure 3-12. This equation assumes solid body motion with no consideration of fluids surrounding it. It also assumes that no forcing function continues to act on the “spring system”, and that the stiffness k_e used is an effective stiffness of the debris and structure, determined assuming springs combined in series.

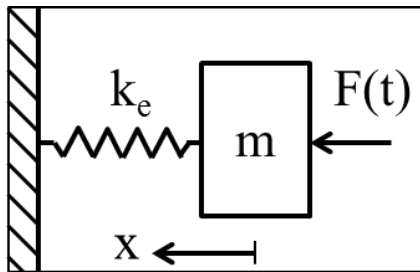


Figure 3-12: Spring System Assumption

Eq 18 yields a force acting on the body equal to the velocity multiplied by the square root of the product of the stiffness constant and mass of the debris, shown in Eq 19 below. Since the building is much stiffer than the debris, it is often assumed that the effective stiffness is equal to the stiffness of the debris, as obtained through impact testing.

$$F = u\sqrt{k_e m} \quad \text{Eq 19}$$

3.5.5.4 Discussion on Added Mass Term

Haehnal and Daly (2002) proved all three methods to be equivalent assuming the forcing function, $F(t)$, to be sinusoidal in the impulse-momentum approach. However, due to the difficulty of estimating impact time, Δt , and stopping distance, Δx , the constant stiffness approach was deemed as the most feasible method for determining impact forces for specific debris sources.

In the determination of the impact forces, it has been shown experimentally that the mass of the debris m should be amplified. The “added mass coefficient” concept is used to incorporate the increase in inertia of an impacting mass due to the motion of the fluid surrounding the mass. The corrected mass, to be used in Eq 17 to Eq 19, thus needs to account for the added mass coefficient.

Using the “added mass coefficient” in Eq 19 is a point of contention. The added mass coefficient was originally derived assuming Newtonian mechanics, where force is proportional to mass multiplied by acceleration. So, while this added mass coefficient can be used consistently in the form of the Eq 17 and Eq 18, the proportionality of force and mass no longer holds in Eq 19.

Experimental studies on the orientation of the debris with respect to the structure, at the point of impact, have shown discrepancies in the added mass coefficient values. In Haenal and Daly (2002), logs with an orientation parallel (0°) to the direction of flow, as

shown in Figure 3-13, had an added mass coefficient of zero despite that 0° orientation produced the largest impulse forces. Forces of logs at an angle of 90° to the structure produced impact forces smaller than the logs angled at 0° ; however, the authors concluded this was due to flexural deformations in the log. If the impact were to occur on a wall where flexural deformation would be reduced then it may not be correct to assume the maximum force occurs at a 0° orientation and that the added mass coefficient could be assumed zero/negligible.

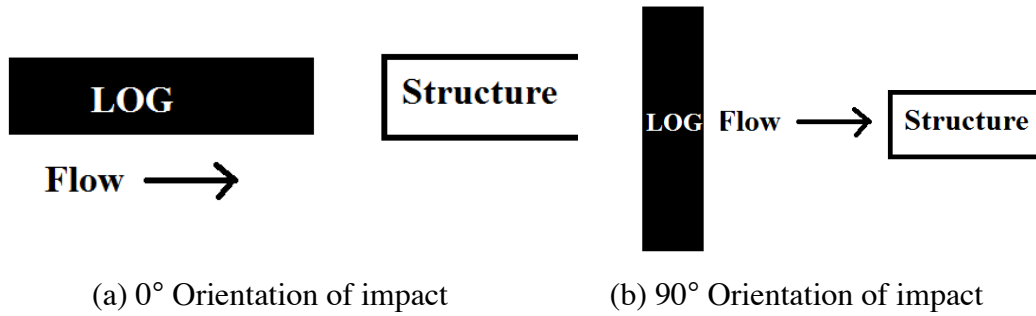


Figure 3-13: Orientation of Impact (Haehnel & Daly, 2002a)

Large-scale NEES experiments by Ko (2013) showed that a coefficient could be used to modify the formula for debris impact force; however, it was mentioned that attributing the coefficient to the added mass effect would not accurately describe the process. Debris impact tests conducted In-Air were compared with specimens conducted In-Water by using the same test specimen material, shape, mass and velocity. Ko (2013) found that for the aluminum test specimens the “magnitude of the peak impact force fell within the 90% confidence interval of the In-Water test” or were smaller than the In-Air tests by a greater margin. The tests also consistently observed an increase in impact duration in the In-Water test. It is also interesting to note that the non-structural mass did not produce a significant effect on measured peak impact forces for neither the In-Air nor In-Water cases. Thus, in equation Eq 20 by Ko (2013), a hydraulic coefficient C_H is used and the mass is the mass of debris only.

$$F = C_H u \sqrt{k_e m} \quad \text{Eq 20}$$

where C_H is a hydraulic coefficient, typically ranging between 1.1-1.4, based on data from the experiments conducted by Ko (2013).

FEMA P-646 uses the same definition for the added mass coefficient as Haenel and Daly (2002), where the added mass coefficient remains inside the square root, since FEMA adopted the constant stiffness equation for estimating the impact forces. This document also provides assumptions for the mass and stiffness of a log assuming parallel

orientation. Furthermore, it assumes a mass coefficient equal to 2 for all debris oriented at 90°.

3.5.6 Jamming

The jamming effect of debris on a structure, also known as the damming effect, increases the surface area exposed to the flow, thus increasing the hydrodynamic force. This force follows after the initial impact force of the debris. FEMA P-646 defines this force using Eq 10, but replacing the width of the structure with the width of the debris, to account for the additional force due to the jammed debris.

3.5.7 Maximum Total Force

The forces given above correspond to maximum forces. Obviously, their maximum values are not likely to occur simultaneously (Lloyd & Rossetto, 2012). Time dependent calculations of force component for building design have been developed by Asakura et al. (2002) and Fujima (2009b).

3.5.7.1 Asakura et al, 2002

Asakura et al. (2002) proposed an empirical formula for the total pressure due to tsunami waves, not considering debris. The equation for pressure as a function of height above ground level is the larger of Eq 21 and Eq 22:

$$P(y) = (5.4\eta_{max} - 4y)\rho g \quad \text{Eq 21}$$

$$P(y) = (3\eta_{max} - y)\rho g \quad \text{Eq 22}$$

where the maximum total force must be positive, and where η represents the maximum inundation depth, ρ is the density of water, y is the height of the position of interest above ground level, and g is the acceleration due to gravity.

3.5.7.2 Fujima et al. 2009

Empirically correlating the total force proportionally to the hydrodynamic force definition shows less scatter than correlating the total force to the hydrostatic force (Fujima et al., 2009b). Fujima proposed equations for the total maximum force with respect to the ratio of maximum inundation depth, η_{max} , to the distance from the shoreline, D ; however, these parameters require detailed information provided by numerical models which may not be available for all sites of interest. Using the formula proportional to the hydrodynamic force, the maximum tsunami wave force is defined with safety factors in Eq 23 for $\frac{\eta_{max}}{D} < 0.05$ (far from the shore) and Eq 24 for $\frac{\eta_{max}}{D} > 0.05$ (near the shore):

$$F = 1.3\rho B_1 \eta_{max} u_{max}^2 \quad Eq\ 23$$

$$F = 3.3\rho B_1 \eta_{max}^2 \quad Eq\ 24$$

In both Eq 23 and Eq 24, ρ is the density of the water, B_1 is the width of the structure perpendicular to the wave front, η_{max} is the maximum depth of tsunami inundation at that location, and u is the maximum flow velocity. Note that this equation has included safety factors (1.733 and 1.833 respectively) and the parameters used are for maximum depth and maximum velocity since those are typically more readily available than the optimized maximum moment flux, although they do not occur at the same time.

3.5.7.3 Total Force Time Series

Total force time plots have been conducted for different laboratory set-ups. These setups either have a surge, a bore, or a series of bores. The experiments also use land structures such as a circular column, a square column, or a wall. The figures below estimate the different effects produced by the various forces over time. The dashed line represents the capacity of the structure to resist against sliding. The decrease in capacity

can generally be attributed to the buoyancy force reducing the resistance of the structure to sliding and overturning.

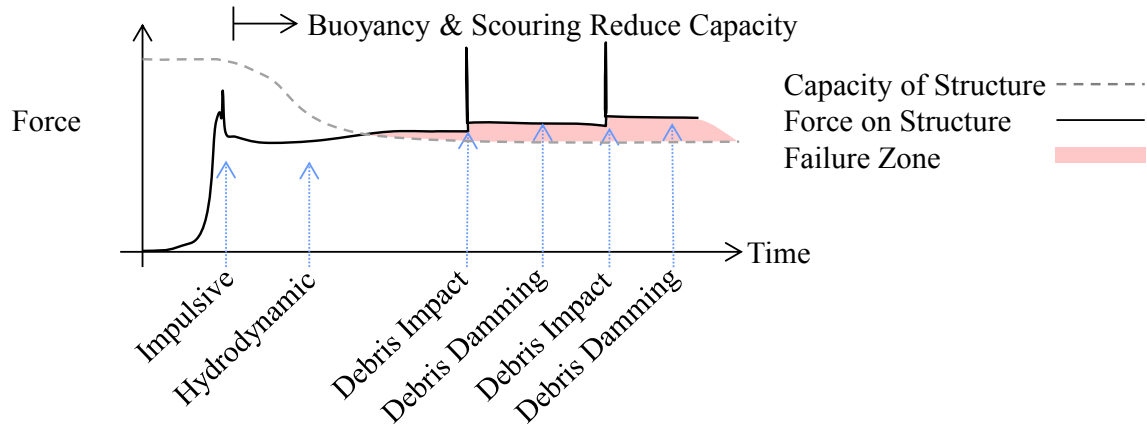


Figure 3-14: Hypothetical Total Force Time Series for Rectangular Structure

In Figure 3-14, the impulsive force from a bore initially affects the structure and then subsequently develops the hydrodynamic force. Here it is assumed that a structure has been inundated prior to the tsunami arrival; otherwise, there would be no impulsive force. This case also assumes that the building is not very wide and that flow will develop around the entire building.

In the case of a very wide/long building or a U-shaped building, the water may not fully envelop the structure and in this intermediate time before the development of the hydrodynamic force, the hydrostatic force of the water accumulating before the structure may increase until water reaches the leeside of the building and a quasi-steady flow is developed. This increase in force may be greater than the initial impulsive force and would be more similar to the case of a wall in laboratory experiments, rather than a column. An example of the hypothesized case with a U-shaped building is shown in Figure 3-15.

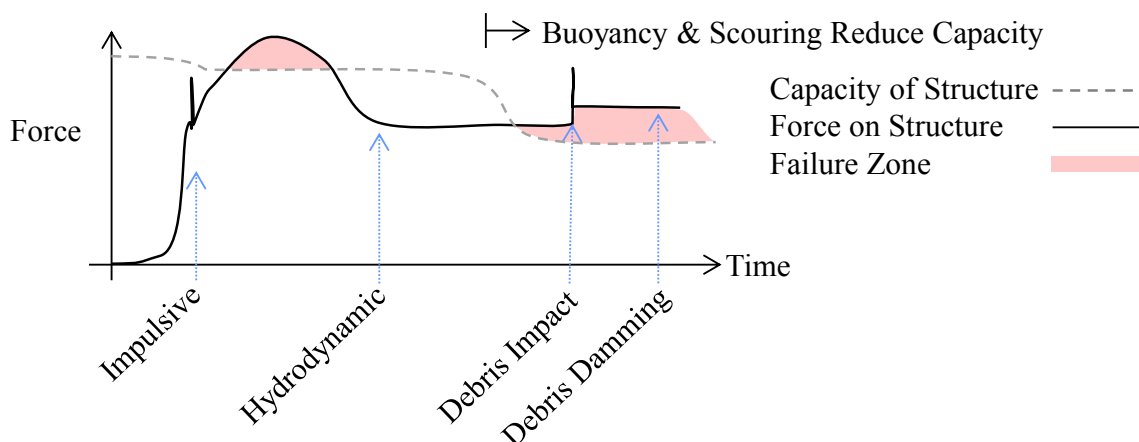


Figure 3-15: Hypothetical Total Force Time Series for U-shaped Structure

3.5.8 Tsunami Force Combinations

Currently, FEMA P-646 (2012) recommends discusses the potential worst-case scenarios for estimating total tsunami forces. In all scenarios, it is advised to consider the buoyant force as it will reduce the capacity of the structure to resist sliding and overturning forces. The following three scenarios summarize the force combinations:

1. buoyant force, hydrodynamic force, and impulsive force
2. buoyant force, hydrodynamic force, and debris impact force
3. buoyant force, hydrodynamic force, and debris damming force

Scenario 1, as shown in Figure 3-16, describes an impulse force exerted on the most closed off portion of the building and a hydrodynamic drag force exerted on all structural components in the wake of the bore. The building must have some preexisting water in order to produce an impulse effect since a surge does not produce an impulsive force greater than the subsequent hydrodynamic force. Note that an impulsive force and a hydrodynamic force do not occur simultaneously at a given location. Also, the buoyant force is difficult to estimate in this case since the leeward side of the structure will not be fully inundated with water. In Figure 3-16 (a) the most closed off portion of the building is the front face, whereas in Figure 3-16 (b) the most closed off portion of the building is the interior wall. In the latter case, a bore condition still needs to exist in order for the impulse force to be applicable.

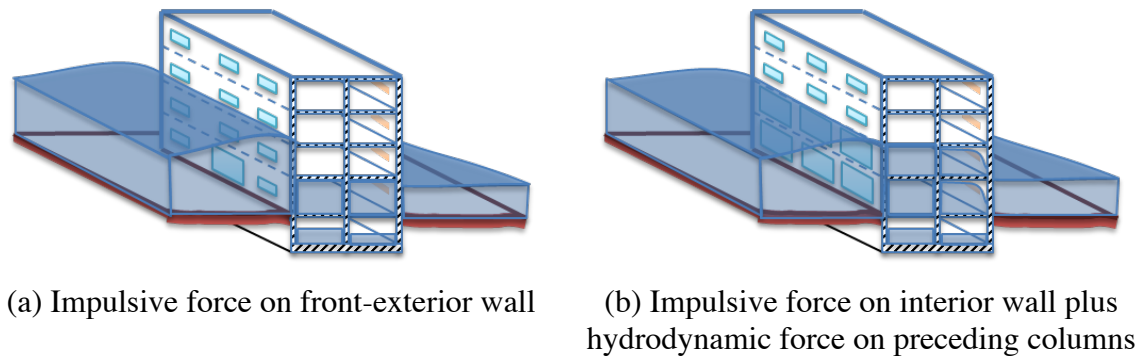


Figure 3-16: Scenario 1 Proposed by FEMA P-646

Scenario 2, as shown in Figure 3-17, describes the debris impact force in conjunction with the hydrodynamic force and the buoyant force. The characterization of the debris and the calculation of a buoyant force are both very uncertain for this scenario. The hydrodynamic force assumes that the building is entirely submerged and also requires an estimate of a coefficient of drag. U-shaped buildings currently have no drag force recommendations in the literature.

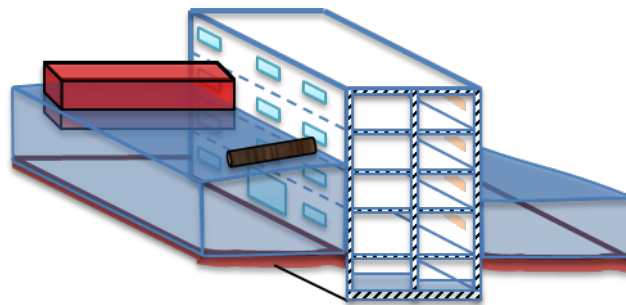


Figure 3-17: Scenario 2 Proposed by FEMA P-646

Scenario 3, as shown in Figure 3-18, describes the debris jamming force from the accumulation of debris over time. This force is an amplification of the hydrodynamic force due to the increased area of the building once debris has accumulated. Therefore, it is important to note that the hydrodynamic force should not be added to the debris damming force, but that the debris damming force is a recalculation of the hydrodynamic

force. However, the debris damming is recommended to “act in the most detrimental location on a structure while hydrodynamic forces act on all other components of the structure” (FEMA P-646, 2012). This is a reasonable approach for considering forces on individual components, such as a column; however, the calculation of forces for the entire building cannot follow this rational since the hydrodynamic force acts on a body entirely submerged in flow.

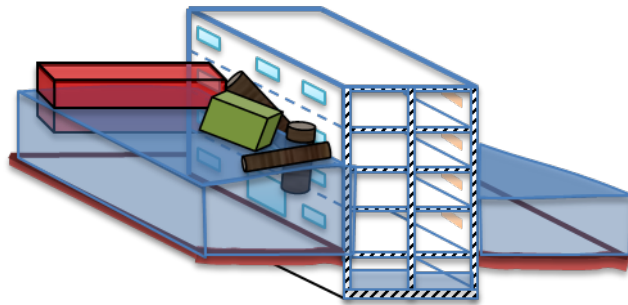


Figure 3-18: Scenario 3 Proposed by FEMA P-646

Inherently, these force combinations have significant assumptions, and are not necessarily based on a time history analysis of the forces. Thus, a more rational method to determine load combinations is needed. The consideration of additional loading scenarios should be addressed to insure that a critical tsunami force combination is not being overlooked. Figure 3-19 shows an example of different time intervals. The hydrodynamic force is only applicable in (b) and (c) while, in Figure 3-9 (a) the hydrostatic force is most applicable, especially for wide buildings or U-shaped buildings.

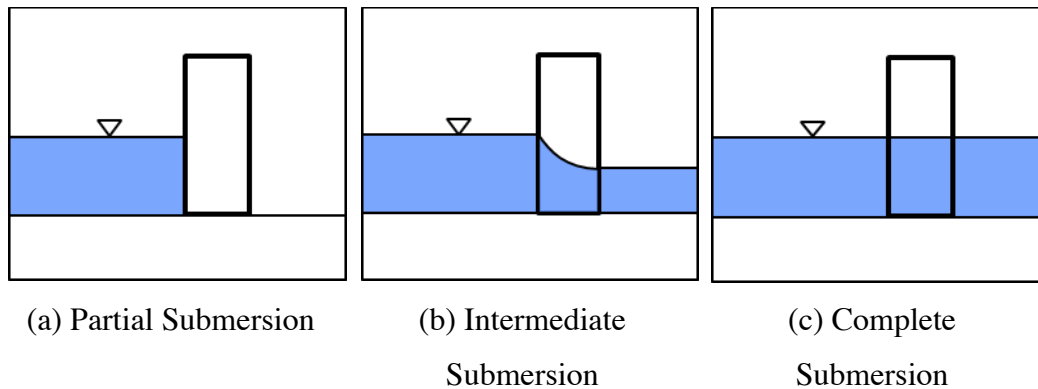


Figure 3-19: Hydrodynamic Force Application – Elevation View

Some important considerations needed when performing force combinations are:

1. Depending if the wave is a leading elevation wave or a leading depression wave, the total force on the structure may differ. The effects of wave type were discussed in Chapter 2.
2. The critical loading condition for a building may be for a scenario when the tsunami wave has inundated only one face of the structure during a sufficiently long initial inundation process prior to reaching the quasi-steady flow condition. This case is especially susceptible for a large-size building with a U-shape, facing the shoreline where the open side takes in tsunami flow. In such a case the hydrodynamic force would not yet be applicable for inclusion in force combinations.
3. It is important to consider the impulsive force when the location of interest is previously flooded due to the steep front of such a bore; it is duly important to note that impulsive forces are not great when the site of interest is initially dry due to the shallow angle of the surge front (Yeh, 2007).
4. Forces caused by debris impact or damming are always important to consider given a source of debris exists and also the water depth is substantial enough to carry the debris.

3.6 Dimensions, Shape and Orientation

Building shape and orientation may amplify force estimations and wave heights. For rectangular buildings, FEMA CCM (2003) has included a table for drag coefficients based on different width to depth ratios. U-shaped buildings open to the direction of flow may experience higher than expected wave forces while buildings with breakaway windows/walls may experience force alleviation. Figure 3-20 illustrates the concept of a U-shaped building.

3.6.1 U-Shaped Buildings

A high water level on the front face, as opposed to the water level on back face, of a building may exacerbate forces in a U-shaped building where the water would funnel into the “U” of the building and not reach the back of the building for a longer time to flow along the dimension B_2 and then subsequently along B_1 , as shown in Figure 3-20, than it would with a rectangular or circular shaped building. This time, Δt , may be sufficiently large for very wide buildings and may potentially produce the critical loading condition due to the accumulation of water within the “U” without a counterbalancing pressure on the leeward side of the building.

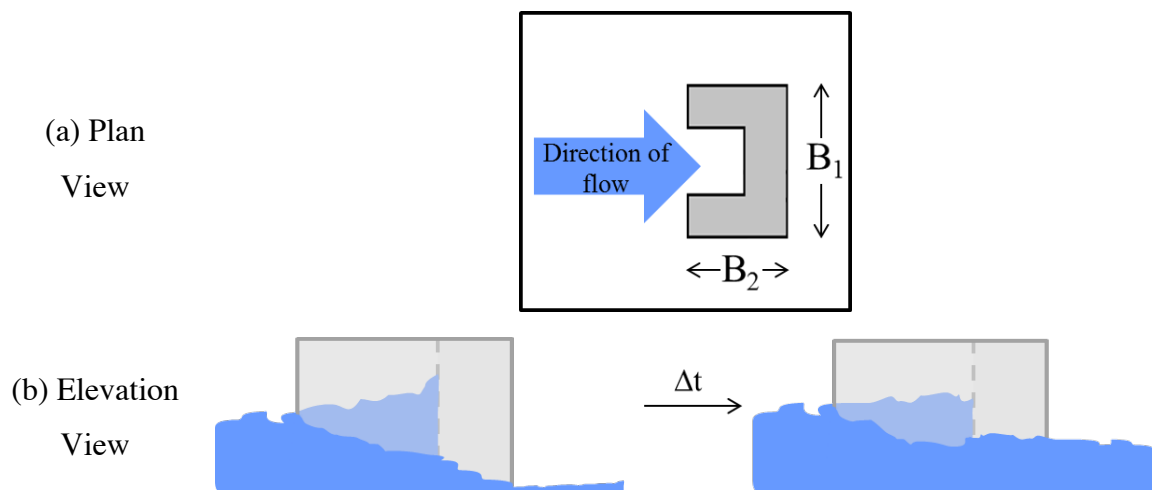


Figure 3-20: “U-Shaped” Building

Okada et al., (2006) reported that Nakano and Park (2005) conducted extensive surveys in Sri Lanka and Thailand after the 2004 Sumatra earthquake and it was found that U-shaped building experienced more damage than rectangular shapes under the equivalent inundation conditions. The researchers correlated the damage to the simplified formula proposed by Asakura (2002), shown in Eq 25.

$$F = \frac{1}{2}(\alpha\eta)(\alpha\rho\eta g) \quad \text{Eq 25}$$

where ρ represents the density of seawater, g represents the acceleration due to gravity, η represents the maximum depth of incoming tsunami runup. Damage correlations reported α values greater than 3 for U-shaped buildings, where other shapes experienced α values less than 3. Causes of this may be due to obstruction of flow, rapidly accumulating water depths, or may be associated with a resonance effect (see Chapter 2), similar to a shock wave in an enclosed room.

3.6.2 Breakaway Windows/Walls

Breakaway windows and walls provide substantial force alleviation for a building (Dalrymple & Kriebel, 2005; Lukkunaprasit, Chinnarasri, Ruangrassamee, & Weesakul, 2008; Yeh et al., 2013), however, the appropriate “efficiency” of designing breakaway windows is not known with much certainty. Since force is proportional to area, the reduced area from windows “breaking away” reduces the force exerted on the structural component. The reduction in force can then be attributed to two parts: (i) the reduced area and (ii) the presence of water entering the building. The presence of water entering the building counteracts the “pressure on the inside of the upstream panel” (Lukkunaprasit et al., 2008). The counteracting pressure on the inside of the upstream panel was reported to have a lag time of about 0.5 seconds to 0.7 seconds. The proportionality of area reduction and force reduction can be understood by the 1-D momentum equation shown below in Eq 24, where ρ represents the density of the fluid, u_1 represents the fluid velocity entering into the control volume, $u_{1,2}$ represents the fluid velocity entering and exiting

the control volume respectively, $A_{1,2}$ represents the area of the fluid entering and exiting the control volume, respectively, and $P_{1,2}$ represents the pressure on the surface of A_1 and A_2 respectively.

$$F = (\rho u_2^2 A_2 - \rho u_1^2 A_1) + (P_2 A_2 - P_1 A_1) \quad \text{Eq 26}$$

Breakaway windows and walls are most effective “inline” with a flow path in and out of the building. One example of this is the buildings in Rikuzpa-Takata, Japan, shown in Figure 3-21: . Two flat and thin apartment buildings are oriented with the most surface area facing the incoming ocean, yet despite their orientation to the ocean, the buildings remained standing after the tsunami, most likely due to the force alleviation from the breakaway windows.



Figure 3-21: Example of Breakaway Walls in Rikuzpa-Takata, Japan (Photo courtesy of Harry Yeh)

Lukkunaprasit (2008) conducted small-scale testing with 0%, 25%, and 50% openings through a rectangular building. Figure 3-22 compares the percent of total force reduced based on the percent opening in the structure. The dashed line in the figure represents the “100% efficiency” of the opening, which means a 1:1 proportionality between the reduction in area and the reduction in force. Figure 3-22 shows that the force from smaller wave heights is alleviated by openings more efficiently than larger wave heights. However, the authors noted in regard to the 30 mm wave height that

measurements of very small wave heights produce more significant errors.

Further testing could be done to reduce the uncertainty of the effects of breakaway windows/walls. Even though force is assumed to be proportional to area perpendicular to flow, the “efficiency of the opening” means that only a portion of the opening is effective in alleviating force from flow.

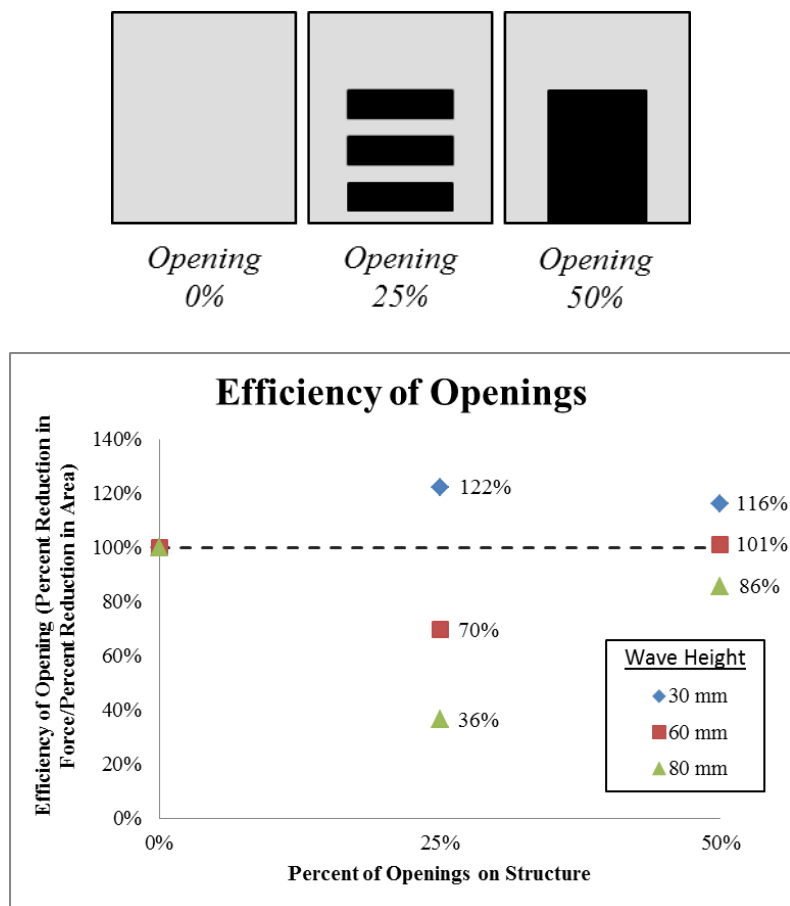


Figure 3-22: Effects of Openings on a Structure. Data Source: Lukkunaprasit (2008)

Another added benefit from breakaway windows/walls is that the inflow of water into the building relieves buoyant forces. However, added pressure from the load of water on the floor may cause damage or additional axial loads to columns; nonetheless, this is only the case if the lower floors are not fully inundated and, furthermore, the increased load helps to stabilize the building in a global consideration of overturning and sliding.

One other concern for using reduced forces based on breakaway windows and walls is the accumulation of debris which may block flow and disable the effects of a breakaway window or wall. This can be accommodated with the use of efficiency terms.

4 REVIEW OF TSUNAMI VERTICAL EVACUATION BUILDING GUIDELINES

Design guidelines to describe tsunami loading on a building have been established in many parts of the world. These guidelines use simplified, applicable formulae based on theory, empirical laboratory studies, and lessons learned from observed damage after a tsunami event. The various tsunami forces acting on a building are characterized as a function of velocity and inundation depth. There are a few discrepancies between definitions of the basic inputs (velocity and height) that arise in most guidelines to describe different physical scenarios (i.e. a bore, surge, or still-water) and also because of the simplification of equations for convenient use in design. These discrepancies were discussed in detail in Chapter 3.

Code provisions should balance conservatism and economy of designs based on the probability of the occurrence and magnitude of the hazard. On one hand, designs cannot be too robust that the expense renders the design infeasible; in such a case, the tsunami evacuation building will not be built. On the other hand, if code provisions are not stringent enough, safety and lives may not be protected and, in fact, inadvertently put at risk. This drives the need for reduced levels of uncertainty and smaller safety factors. Uncertainty in tsunami design is especially difficult to avoid because tsunami runup can vary up to 100% within even two kilometers based on very small changes in local topography/bathymetry or land features as shown in Figure 4-1 (Yeh, 2009). The location and magnitude of the source earthquake, bathymetry and local terrain all add uncertainty but this can be minimized with numerical modeling to incorporate their effects.

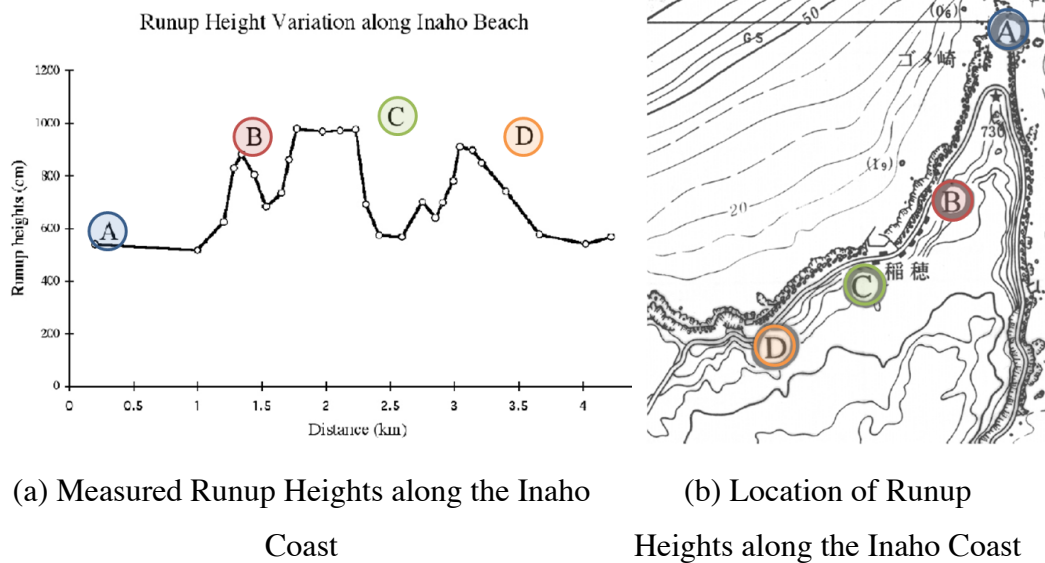


Figure 4-1: Example of Significant Variation of Runup Heights: 1993 Okushiri Tsunami (Source: Yeh, 2009)

The extreme variability of tsunami forces based on very small changes in location, as shown on Figure 4-1a, identifies an increased need for design consideration on a site-specific basis, factoring in local bathymetry/topography and other terrain effects.

4.1 United States

The United States has developed a number of guidelines to assess tsunami loads on a structure, although currently none are required by the building code. However, the future version of ASCE/SEI 7 will incorporate tsunami loading code provisions (Chock, 2012a). Currently, major design guidelines developed in the US include:

- Federal Emergency Management Agency (FEMA) P-646: Guidelines for Design of Structures for Vertical Evacuation from Tsunamis (2008; 2012),
- FEMA Coastal Construction Manual (2003)
- The City of Honolulu Building Code (2013) based off of the work by Dames and Moore (1980), and other miscellaneous tsunami design reports.

4.1.1 Federal Emergency Management Agency, P-646

In 2012, the Federal Emergency Management Agency (FEMA) produced the second edition of Guidelines for Design of Structures for Vertical Evacuation from Tsunamis (FEMA P-646, 2012); the revisions are minor, relieving some over-conservatism in its original version (FEMA P-646, 2008). The guidelines provide formulae and example calculations to determine the maximum forces produced by the different type of wave forces. The forces are hydrostatic, hydrodynamic (drag), impulsive, debris impact, debris damming, and buoyant force. However, no time dependent force combinations are specified to incorporate the different types of tsunami forces. However, FEMA P-646 (2012) does provide a series of load combinations with Dead, Live, Tsunami Loads, and Live loads specifically for additional refugees using Strength Design Load Combinations.

The tsunami force equations evaluate maxima of each type of wave loading, without specifying their probability of coincidence or any physical interpretation as to when these occur simultaneously. The latter is important to understand how these tsunami forces should be combined. For example, still water exerts a hydrostatic force on the side of a building, then an incoming wave exerts an impulsive force for a short period of time, and then the hydrodynamic force is the major force proponent until another wave or debris impacts the structure. Therefore, time-varying loading (Lloyd & Rossetto, 2012) and building shape considerations should be researched further. The net force caused by discrepancies between water depths around the large building is not addressed.

4.1.2 City of Honolulu Building Code (Dames & Moore, 1980)

The 2007 Honolulu Building Code has provisions based on the a report by Dames and Moore (1980), *Design and Construction Standards for Residential Construction in Tsunami-Prone Areas in Hawaii* and defined four tsunami forces. The forces are hydrostatic, hydrodynamic, impact, and soil loads. Soil loads result from the deposition of sediment against the structure; however, the code also makes a discussion of scour and the reduction of bearing capacity of the soil due to saturation. The code recommends the application of all the forces alone or in combination “in such a manner that the combined

effect will result in maximum loads and stresses on the structure and members”. No specific load combination is specified. Interestingly, the code specifies areas where a bore condition is likely to exist and all other locations are to be considered for inundation resulting from a non-bore condition. The code also uses the same equation for surge force as Asakura (2002) in Eq 25.

4.1.3 United States Nuclear Regulatory Committee

The United States Nuclear Regulatory Committee (USNRC) produced a report *Tsunami Hazard Assessment at Nuclear Power Plant Sites in the United States of America* (Prasad, 2009). The report discusses near-field and far-field tsunamis and cites expressions for the hydrostatic force, hydrodynamic force, and impulsive wave force on a vertical pile or column, impulsive wave forces on vertical walls, debris impact effects, and buoyant forces. This document references Yeh et al. (2005) and the FEMA Coastal Construction Manual (2003). The report also discusses scour and sediment deposition.

4.2 Japan

Japan first developed tsunami countermeasures in 1933 after experiencing the 1933 Showa Great Sanriku Tsunami and the 1896 Meiji Great Sanriku Tsunami, claiming 3,000 and 22,000 lives, respectively. A research group, the Council on Earthquake Disaster Prevention of the Ministry of Education, developed 10 countermeasures (Shuto & Fujima, 2009) quoted below:

1. *Relocation of dwelling houses to high ground. This is the best measure against tsunami.*
2. *Coastal dikes: Dikes against tsunamis may become too large, and financially impractical.*
3. *Tsunami control forests: Vegetation may damp the power of tsunamis.*
4. *Seawalls: These could be effective for smaller tsunamis.*

5. *Tsunami-resistant areas: If the tsunami height is not so high in a busy quarter, solid concrete buildings are to be built in the front line of the area.*
6. *Buffer zone: Dammed by structures, a tsunami inevitably increases its height. In order to receive the flooding thus amplified, rivers and lowlands are to be designated as buffer zones to be sacrificed.*
7. *Evacuation routes: Roads to safe high ground are required for every village.*
8. *Tsunami watch: Because it takes 20 minutes for a tsunami to arrive at the Sanriku coast, we may detect an approaching tsunami and prepare for it.*
9. *Tsunami evacuation: The aged, children and weak should be evacuated to safe higher ground where they could wait for about one hour. Ships, more than a few hundred meters offshore, should move farther offshore.*
10. *Memorial events: Holding memorial services, erecting monuments, etc. may help keep events alive in people's mind.*

4.2.1 Cabinet Office Guidelines

In 2005, the Japanese government office produced guidelines for the evaluation of tsunami forces on building structures. The guidelines were proposed for the design of tsunami evacuation buildings. This document was a continuation of the Tsunami Disaster Prevention Countermeasures in Local Disaster Prevention Planning from 1997. The guidelines use an empirical formula proposed by Asakura (2002) where the maximum tsunami wave is three times the inundation depth with a triangular pressure distribution as shown in Figure 2-2, and described by Eq 25. The parameter three was assumed as the alpha value in Eq 25 because it was the “dividing line between damage and no damage” for reinforced concrete buildings (Okada et al., 2006).

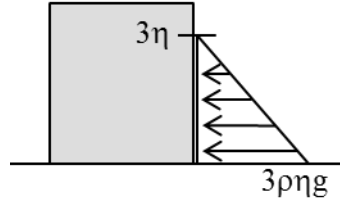


Figure 4-2: Asakura (2002) Model Definition Estimating Total Tsunami Force

In the development of the Cabinet Office Guidelines (2005), other equations were proposed, but these were found to produce forces identical to that of Asakura. Ultimately, the equation proposed by Asakura was utilized for simplicity (Okada et al., 2006). It is noted that forces produced by debris damage need to be considered in addition to the force described by Eq 25. Furthermore, the author pointed out the importance of flow velocity for the estimation of forces and recommended using equations that include velocity if velocity information is available for the site of interest.

Asakura's formulation grossly simplifies the flow conditions by calculating the forces based only on an inundation depth. Asakura's formula was between 1.125 to 2 times higher when compared to the hydrodynamic equation shown in Eq 9. Implicit in this comparison is the assumption of a Froude number, shown in Eq 27, which was taken as 2, and a coefficient of drag between 1.1 and 2. This simplification, and its implicit assumptions for the coefficient of drag and velocity (Froude number), may grossly over-estimate forces in circumstances with slow velocities and may under-estimate forces in circumstances with irregular shapes, such as U-shaped buildings, as was shown by Okada et al. (2006).

$$F_r = \frac{u}{\sqrt{gh}} \quad \text{Eq 27}$$

One of the equations compared to Asakura's formulation was proposed by Ohmori and his colleagues (2000) and did include building width and length as inputs for the force equations. Their research had included a time history analysis that evaluated a

maximum force based on the hydrodynamic, inertia, impulsive, and hydraulic gradient forces. Although it is considered equivalent to Asakura, the paper did not clearly specify the building shape assumptions necessary for equivalency.

4.2.2 Ministry of Land, Infrastructure, Transportation and Tourism

The Ministry of Land, Infrastructure, Transportation and Tourism (2011) composed an interim guideline for the design and construction of tsunami evacuation buildings that allows for the reduction of forces based on the presence of a breakwater structure and the distance from the shoreline or river. A breakwater is a structure constructed in the near-shore water for the purpose of coastal protection, similar to a seawall, although seawalls are constructed along the shoreline in order to prevent wave intrusion inland. Breakwaters and seawalls are built to promote tsunami wave attenuation. The new formulation modifies the formula by Asakura by changing the “three times the inundation depth” to a water depth coefficient “ α ” instead of “3”. The parameter is reduced to “2” if protected by a breakwater shelter and “1.5” if protected by a breakwater shelter and more than 500 m from the seashore or river (Fukuyama et al., 2013). In the discussions provided by Fukuyama et al. (2013) breakwater shelters that can be expected to reduce the forces produced from the waves included upright seawalls, including those at the mouth of the bay and tide embankments that are significantly high, such as a coastal dike. A coastal dike is a mound-like structure along the shoreline used for coastal flood prevention.

4.3 Other

A number of other tsunami guidelines have been developed around the world. Multinational groups have been established to provide a unified network of information dissemination and progress. Japan has a government program, Science and Technology Research Partnership for Sustainable Development (SATREPS) that promotes international joint research (Yamazaki & Zavala, 2013). The United Nations Educational, Scientific and Cultural Organization (UNESCO) disseminates international tsunami

information, hazard maps and warnings from their International Tsunami Information Center (World Bank & GFDRR, 2012).

4.3.1 **Palermo, Nistor, Nouri, & Cornett**

Canada has experienced many tsunamis, but only one led to the loss of 28 lives in 1929 by the Grand Banks earthquake (Clague et al., 2003). However, Canadian researchers have contributed to the discussion on tsunami design forces.

A paper in the Canadian Journal of Civil Engineering titled, *Tsunami Loading of Near-Shoreline Structures: a primer* (Palermo et al., 2009) was written by researchers from the University of Ottawa and the Canadian Hydraulics Center of the National Research Council. In it the authors discuss the lack of building design considerations for a potential tsunami from the Cascadia Subduction Zone, the same tectonic plate that worries researchers on the west coast of the United States (Palermo et al., 2009).

4.3.2 **World Bank**

The Global Facility for Disaster Reduction and Recovery (GFDRR) at the World Bank supported the set of “Knowledge Notes” produced by the Earthquake Engineering Research Institute (EERI) (World Bank & GFDRR, 2012). The structural section defines how to design and build breakwater walls and prevent scour. The document referenced the total force formulations used by the Japanese government based on the equation proposed by Asakura (2002).

4.3.3 **The World Association for Waterborne Transport Infrastructure**

The World Association for Waterborne Transport Infrastructure produced a report titled, *Mitigation of Tsunami Disasters in Ports* (2010). In it the authors describe the history of tsunamis all over the world, harbor resonance, and flow velocities. The forces considered are tsunami wave pressure on a wall and on a single structural element, such as a column, and also debris impact forces.

4.4 **Conclusion**

A review of the guidelines has shown that no force combination has been consistently used and the notation characterizing tsunami waves is not unified. Points of consistency do exist, such as the individual force determinations for the hydrostatic and

buoyant forces. However, by and large, most guidelines have used their own experimental methods to estimate tsunami forces.

5 PROPOSED DESIGN RATIONALE

This thesis has presented several sources of uncertainty in Tsunami Hazard Analysis (Chapter 2), Tsunami Structural Analysis (Chapter 3), and in the existing guidelines used in Tsunami Building Design (Chapter 4). In this chapter, a new design rationale is proposed for Tsunami Vertical Evacuation Buildings.

Figure 5-1 shows the proposed design rationale. The first step in the design rationale is to assess the flow conditions at the site based on the wave source and subsequent wave forms and local conditions. An analysis of debris and scour should also be included in this portion of design. The second step in the rationale is to perform a Tsunami Structural Analysis to combine the tsunami forces into maximum tsunami forces/moments as discussed in “Section 3.5 Forces” and to determine story drifts. The third and final step is to apply these building forces, moments, and drifts in the building design. This may be an iterative process if the beams/columns need to be resized, any additional breakaway windows/walls need to be added, or any changes in the foundation need to be made. Furthermore, the failure modes addressed by this level of analysis are global sliding and rotational failures as well as component collapse.

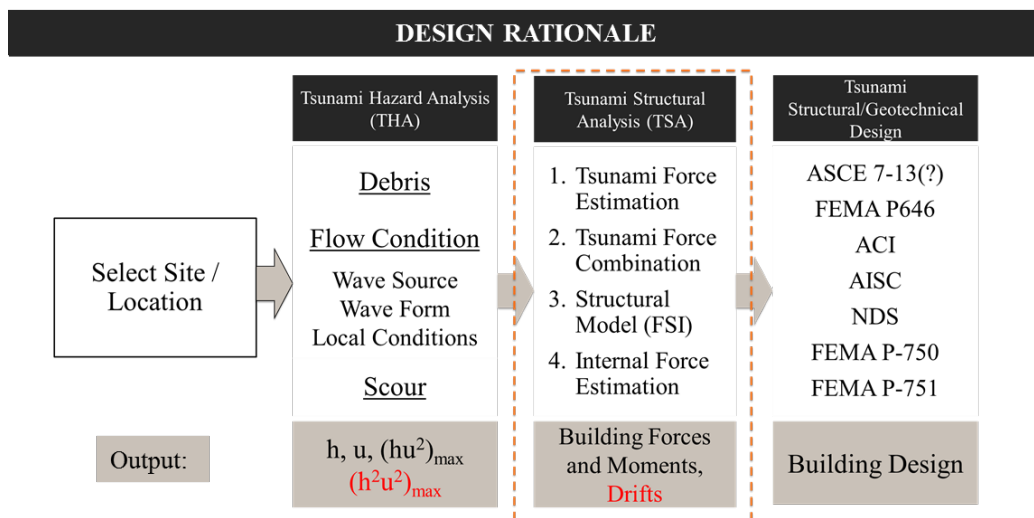


Figure 5-1: Design Rationale for Tsunami Vertical Evacuation Buildings

The Tsunami Structural Analysis (TSA) methodology proposed is based on a three-tiered system for determining building forces, moments, and drifts due to the tsunami loadings. The tiers are shown in Figure 5-2.

Tiered Approach to Tsunami Force Estimation			
Tier 3			Site-specific (FSI) Numerical Simulations
Tier 2		FEMA P-646 $h_{\max} u_{\max} (hu^2)_{\max}$	ASCE 7 $h, u_{\{\frac{1}{3}h, \frac{2}{3}h, \max, \frac{2}{3}h_{\text{receding}}\}}$
Tier 1	Asakura (2002) h_{\max}, a	FEMA P-646 R, z	

Figure 5-2: Tiered Approach to Tsunami Force Estimation

For the status quo, Tiers 1 and 2, require depth and velocity input parameters, and the National Tsunami Hazard Mitigation Program (NTHMP) could potentially provide these. NTHMP is working to produce inundation maps based on credible worst-case scenarios (FEMA P-646, 2012). These include maps of maximum inundation depth and velocity; although, the numerical models also typically produce parameters of flow depth, velocity, acceleration, and momentum flux. These maps, based on site-specific numerical models, reduce the uncertainty of the tsunami wave runup pattern; however, they do not account for uncertainties in combining the tsunami forces on the structure nor additional requirements of coseismic, debris, and soil instability.

Each higher tier decreases the uncertainty associated with force estimation. Uncertainties when predicting tsunami forces, as discussed in this thesis, include the following:

1. tsunami runup pattern
 - a. tsunami source event
 - b. wave form

- c. bathymetry/local terrain
- 2. additional force requirements
 - a. coseismic effects
 - b. debris sources
 - c. soil instability
- 3. combination of tsunami forces (i.e. hydrostatic, hydrodynamic, impulsive, etc.)
 - a. building shape effects
 - b. critical flow conditions/forces

When determining loads on the structure, these uncertainties can propagate through the entire Tsunami Hazard Assessment (TSA). An example of calculating forces is shown in the Appendix for Tier 1 and Tier 2 calculations. Given one data source, very large discrepancies between the tiers are shown in the calculations, demonstrating the uncertainty involved in force calculations at these levels. Only once these discrepancies are addressed, will it make sense to review further how to reduce epistemic uncertainty.

5.1 Tier 1 Analysis

Tier 1 analysis only requires the depth of inundation to calculate forces. Using the depth of inundation to determine tsunami forces on a building is the most simplified method of the three tiers. Tier 1 uses a modification of the hydrostatic equation to include dynamic force effects. This is what has been historically done to estimate tsunami forces without numerical models to estimate flow conditions, i.e. flow velocities.

In Tier 1, forces can be estimated using Asakura (2002) equations or the equations developed in FEMA P-646 (2012). The analysis developed by Asakura (2002), and generally accepted by the Japanese Building Research Institute and the Cabinet Office of Japan, is based on only one depth parameter; the analysis was previously discussed in Chapter 3 (see Eq 22). FEMA P-646 also provides a basic analysis using only the runup elevation and elevation of the location of interest, as was shown in Figure 3-4. Although the total tsunami force prediction by Asakura (2002) does not require a load combination, Okada et al. (2006) explicitly stated in the application of Asakura's equation that debris forces need to be considered. Also, discussions are made for reducing uncertainty in the

computation of this total force based on the presence of shielding effects or known flow velocity. In the latter case, it would be considered a Tier 2 analysis. All total force calculations from FEMA P-646 require some form of manual force combination to find the peak total tsunami force.

5.2 Tier 2 Analysis

Tier 2 analysis requires numerical modeling to estimate tsunami height and velocity parameters. The numerical models typically assume an artificial roughness without actually including land features, such as buildings, in the model.

Examples of critical flow parameters required in Tier 2 analysis include the depth at the maximum velocity, the velocity at maximum depth, and the maximum momentum flux parameter $(hu^2)_{max}$. It is recommended herein to include $(h^2u^2)_{max}$ for evaluation of the peak overturning moment. In the upcoming ASCE 7, the input parameters are expected to be: (i) the maximum height, 1/3 maximum height, 2/3 maximum height, and their corresponding velocities, and (ii) 2/3 height when the water is receding and corresponding velocity. Currently, numerical models can provide these parameters and production of maps including the parameters for coastal communities is being developed by the National Tsunami Hazard Mitigation Program (NTHMP) based on credible worst-case scenario tsunamis. In the case of Alaska and California, credible worse-case scenarios include landslides along with seismic sources (FEMA P-646, 2012). The forces still require a rationale for force combinations and three are provided within FEMA P-646 (2012). This tier removes some of the uncertainty associated with tsunami runup pattern since the velocity term from numerical models can account for these, however, the same uncertainty associated with force combinations and building shape effects, among others, still exists.

5.3 Tier 3 Analysis

Tier 3 analysis would be prepared on a site-by-site basis and would estimate forces directly from an advanced fluid-structure interactions numerical model. These models would incorporate actual buildings and their potential effects, similar to what is

done for wind engineering. This tier of analysis may include time series information on depth and velocity to incorporate in small-scale numerical models for the building of interest. This is recommended for important facilities, such as tsunami vertical evacuation buildings. Currently, this is not commonly done for design of vertical evacuation buildings. The Tsunami Assessment Method for Nuclear Power Plants in Japan (JSCE, 2002) includes some methodology in the process of developing and checking these numerical models, such as using historical tsunamis for comparison and also conducting parametric studies on the input parameters for the numerical models.

The advantage of Tier 3 analysis is the increased certainty in force estimation, which may provide safer and more economical designs. By reducing the uncertainty, factors of safety can be reduced because design forces can be determined with fewer assumptions. If the building can be designed for smaller forces, it may increase the feasibility of coastal communities to build tsunami vertical evacuation buildings. Furthermore, since all of the aforementioned levels of Tiered analysis require numerical modeling at some level to predict inundation or velocity, the assumptions and uncertainties underlying those models as well as comprehensive flow conditions are already included in the numerical models.

Disadvantages to a Tier 3 approach include:

1. Excessive data and computational expertise needed for such models – to have reliable information that can be obtained using LIDAR and other GIS mapping technologies, high resolution terrain models can be developed; however, to incorporate such specific boundary conditions is very computationally expensive.
2. Potential changes in local topography that might have been included in the reduction of forces at the time of analysis – the design is greatly affected by the building surroundings, and land altering events (i.e. tsunamis and earthquakes) have a low probability of occurrence and other sources of change could be managed by the land development permits issued by the city or by including a factor of safety within the design forces. Currently, if any significant changes in the region occur that might produce larger tsunami

forces than originally predicted by the numerical models (before the construction of the building).

3. The site-specific nature of the analysis decreasing the repeatability of designs – the site-specific nature of the analysis is beneficial for accuracy, however, since building design codes can be calibrated after events occur, the complex nature of the numerical model makes it difficult to adjust. This could be addressed in the actual structural design of the building; refer to Figure 5-1 for reference.

Another trade-off that may need to be considered more in depth is the risk of spending portions of the budget on site-specific numerical simulations instead of over-designing the structure to reduce risks. Typically, the costs of numerical simulation are a fraction of building material and labor costs. Furthermore, more economical designs reduce material waste and potentially reduce environmental impacts of construction processes. Thus, it can be concluded that site-specific numerical simulations would be beneficial for the design of vertical evacuation buildings.

6 CONCLUSIONS

Based off of the current body of knowledge, specifically that which was presented in this document, a novel design rationale was proposed that addresses five specific topics that need to be incorporated in future design guidelines. They consist of the following:

1. *Tsunami parameter clarification, including assumptions/applicability of different depth, velocity, added mass coefficients, among other parameters*

Unified notation is important for communication in interdisciplinary topics, especially for design guidelines. In addition, the correct application of each type of force requires clear communication in the guidelines. For example, the hydrodynamic force (drag force) requires flow around the object (i.e. submersion). Furthermore, depth, height, and velocity parameters are currently not well defined. The bore velocity, surge velocity, and receding water velocity are all unique parameters and the associated force effects should be specified accordingly, if possible.

2. *Flow parameter $(h^2u^2)_{max}$ needs to be developed for computing overturning moments with reduced uncertainty*

As discussed in the text, the overturning force has not yet been a major consideration in the design of tsunami vertical evacuation buildings. However, many buildings toppled over in the March 11 tsunami in Japan. Currently, it is recognized that the maximum momentum flux, $(hu^2)_{max}$, occurs at a unique time and is grossly overestimated by multiplying maximum depth and maximum velocity. Overturning moment is a function of $(h^2u^2)_{max}$ and therefore the maximum overturning moment may occur at a different time than the maximum moment flux. It is a recommendation of this thesis to include this parameter in future code provisions, to determine the maximum overturning forces exerted on the building.

3. *Building shape effects, for example for U-shaped buildings, need to be considered in the estimation of drag force coefficients and also in the determination of the most realistic and governing tsunami force combinations*

Building shapes, especially including U-shaped buildings, should be adequately assessed in the determination of forces and loading conditions. Not only does the shape affect the dimensions exposed to wave forces, but it also can change the flow conditions and cause much larger forces than anticipated using inappropriate drag coefficients. The accumulation of water on the front face of U-shaped buildings makes it more susceptible to higher than anticipated forces, especially without breakaway windows; this was shown by Okada et al. (2006) based on extensive field surveys after the 2004 Indian Ocean Tsunami in the areas of Sri Lanka and Thailand. The lack of emphasis on building shape and orientation is an important consideration requiring further investigation.

4. *Identification and applicability of critical flow conditions as well as appropriate force combinations*

Critical flow conditions and force combinations have been recommended by guidelines such as FEMA P-646 and are anticipated in the upcoming release of ASCE 7; however, the significant differences in flow conditions based on local terrain and waveform invite the question of the applicability of all wave scenarios in the force combinations. Applying all scenarios to a building may produce overly conservative design loads that have a low probability of occurrence or, devastatingly, the true flow conditions and tsunami wave forces may exceed those calculated due to the lack of an unconsidered scenario. Thus, over-conservative or potentially unsafe buildings may be designed if only prescribed loading scenarios are used for force calculations. Some level of uncertainty must be accepted with all designs; however, the extreme variability in the tsunami force combinations

based on the input factors can be reduced with site-specific numeric modeling to determine critical flow conditions.

The four topics discussed above are important to mitigate risk in the design of vertical tsunami evacuation buildings and to promote economical designs that are feasible for many communities. For the engineering struggle of balance between affordable and conservative designs, tsunamis pose the added difficulty of highly variable flow environments. Buildings publically promoted as vertical evacuation buildings have a great potential for saving lives and therefore a high level of importance. This thesis outlines various levels of analysis of tsunami forces on a building and can now recommend the use of a tiered structure for analysis and a new design rationale for civil structures. Lower tier levels of analysis may be acceptable for individual designs against tsunamis, but structures promoted publically as vertical evacuation buildings should include site-specific numerical simulations to determine peak tsunami force combinations. Recognizing the distinct levels of uncertainty in design promotes the use of more advanced analysis tools and a better design.

7 REFERENCES

- Árnason, H. (2005). *Interactions between an incident bore and a free-standing coastal structure*. UMI Dissertation Services.
- Arnason, H., Petroff, C., & Yeh, H. (2009). Tsunami Bore Impingement onto a Vertical Column. *Journal of Disaster Research*, Vol.4, No.6.
- Asakura, R., Iwase, K., Ikeya, T., Takao, M., Kaneto, T., Fujii, N., & Ohmori, M. (2002). *Tsunami Wave Force Acting on Land Structures*.pdf.
- ASCE-COPRI-PARI Coastal Structures Field Survey Team. (2013). *Tohoku, Japan, Earthquake and Tsunami Of 2011: Survey of Coastal Structures*. ASCE Publications.
- Bernard, E. N. (2005). The US National Tsunami Hazard Mitigation Program: A Successful State—Federal Partnership. In *Developing Tsunami-Resilient Communities* (pp. 5–24). Springer. Retrieved from http://link.springer.com/chapter/10.1007/1-4020-3607-8_1
- Breaker, L. C., Norton, J. G., Carroll, D., & Murty, T. S. (2009). Comparing sea level response at Monterey, California from the 1989 Loma Prieta earthquake and the 1964 great Alaskan earthquake. *Science of Tsunami Hazards*, 28(5), 255.
- Cabinet Office. (2005). The Guideline Concerning a Tsunami Refugee Building, etc. Retrieved from <http://www.bousai.go.jp/jishin/chubou/index.html>
- Charvet, I. (2012). *Experimental modelling of long elevated and depressed waves using a new pneumatic wave generator*. UCL (University College London). Retrieved from <http://discovery.ucl.ac.uk/1343903/1/1343903.pdf>
- Chock, G. (2012a). ASCE 7 and the Development of a Tsunami Building Code for the U.S. Presented at the 14th U.S.-Japan Workshop on the Improvement of Structural Design and Construction Practices, Maui, Hawaii. Retrieved from https://www.atcouncil.org/files/ATC-15-13/Papers/06_CHOCKpaper.pdf
- Chock, G. (2012b). ASCE 7 Tsunami Loads and Effects Code Development. Presented at the 14th U.S.-Japan Workshop on the Improvement of Structural Design and Construction Practices, Maui, Hawaii. Retrieved from https://www.atcouncil.org/files/ATC-15-13/Papers/06_CHOCKpaper.pdf
- City of Honolulu. (2013). *City of Honolulu Building Code*. Retrieved from <http://archive.org/details/gov.hi.honolulu.building>
- Clague, J. J., Munro, A., & Murty, T. (2003). Tsunami Hazard and Risk in Canada. *Natural Hazards*, 28(2-3), 435–463. doi:10.1023/A:1022994411319
- Cross, R. (1967). Tsunami Surge Forces. *Journal of the Waterways and Harbors Division of the American Society of Civil Engineers*, 201–231.

- Dalrymple, R. A., & Kriebel, D. L. (2005). Lessons in engineering from the tsunami in Thailand. *BRIDGE-WASHINGTON-NATIONAL ACADEMY OF ENGINEERING*-, 35(2), 4.
- Dames & Moore. (1980). *Design and Construction Standards for Residential Construction in Tsunami-Prone Areas in Hawaii*. Washington, D.C.: Prepared for the Federal Emergency Management Agency.
- DOGAMI. (2013). Oregon Geology Fact Sheet: Tsunami Inundation and Evacuation Maps for Oregon. Oregon Department of Geology and Mineral Industries. Retrieved from <http://www.oregongeology.org/pubs/fs/TIM-maps-factsheet.pdf>
- Federal Emergency Management Agency. (2003). *Coastal Construction Manual: Principles and Practices of Planning, Siting, Designing, Constructing, and Maintaining Residential Buildings in the Coastal Environment* (Vol. 1). Reston, Va: American Society of Civil Engineers.
- FEMA P-646. (2012, April). Guidelines for Design of Structures for Vertical Evacuation from Tsunamis.
- Fujima, K., Achmad, F., Shigihara, Y., & Mizutani, N. (2009a). Estimation of tsunami force acting on rectangular structures. *Journal of Disaster Research*, 4(6), 404–409.
- Fukui, Y., Nakamura, M., Shiraishi, H., & Sasaki, Y. (1963). Hydraulic study on tsunami. *Coastal Engineering in Japan*, 6, 67–82.
- Fukuyama, H., Kato, H., Ishihara, T., Tajiri, S., Tani, M., Okuda, Y., ... Nakano, Y. (2013). Structural Design Requirement on the Tsunami Evacuation Buildings. Presented at the 14th U.S.-Japan Workshop on the Improvement of Structural Design and Construction Practices, Maui, Hawaii. Retrieved from https://www.atcouncil.org/files/ATC-15-13/Papers/05_FUKUYAMApaper.pdf
- Geist, E. L. (1999). Local tsunamis and earthquake source parameters. *Advances in Geophysics*, 39, 117–209.
- Haehnel, R., & Daly, S. (2002a). Maximum Impact Force of Woody Debris on Floodplain Structures.pdf.
- Haehnel, R., & Daly, S. (2002b). Maximum Impact Force of Woody Debris on Floodplain Structures.pdf.
- International Council for Science Scientific Committee on Oceanic Research Working Group 107. (2002). *Improved global bathymetry: final report of SCOR Working Group 107* (Vol. 63). UNESCO.
- JSCE. (2002). Tsunami Assessment Method for Nuclear Power Plants in Japan. Tsunami Evacuation Subcommittee, Nuclear Civil Engineering Committee, Japan Society of Civil Engineers (JSCE). Retrieved from http://committees.jsce.or.jp/ceofnp/system/files/JSCE_Tsunami_060519.pdf
- Keulegan, G. H. (1950). Wave motion. *Engineering Hydraulics*, 12–15.

- Ko, H. T. (2013). Hydraulic experiments on impact forces from tsunami-driven debris. Retrieved from <http://ir.library.oregonstate.edu/xmlui/handle/1957/38478>
- Kulikov, E. (2006). Dispersion of the Sumatra tsunami waves in the Indian Ocean detected by satellite altimetry. *Russ. J. Earth Sci*, 8. Retrieved from <http://www.agu.org/WPS/rjes/v08/2006ES000214/2006ES000214.pdf>
- Lloyd, T. O., & Rossetto, T. (2012). A comparison between existing tsunami load guidance and large-scale experiments with long-waves. Retrieved from http://www.iitk.ac.in/nicee/wcee/article/WCEE2012_1092.pdf
- Lo, R. C., & Wang, Y. (2012). Lessons Learned from Recent Earthquakes—Geoscience and Geotechnical Perspectives. Retrieved from http://cdn.intechopen.com/pdfs/28211/InTech-Lessons_learned_from_recent_earthquakes_geoscience_and_geotechnical_perspectives.pdf
- Lukkunaprasit, P., Chinnarasri, C., Ruangrassamee, A., & Weesakul, S. (2008). Experimental Investigation of Tsunami Wave Forces on Buildings with Openings. In *2008 Solutions to Coastal Disasters Conference*.
- Mader, C. L. (2004). *Numerical modeling of water waves*. Crc Press.
- Mohamed, A. (2008). *Characterization of tsunami-like bores in support of loading on structures* (Thesis).
- NAKANO, Y., & PARK, J.-H. (2005). Studies on Lateral Resistance of Structures and Tsunami Load Caused by the 2004 Sumatra Earthquake□: Part 1 Outline of Survey. *Summaries of Technical Papers of Annual Meeting Architectural Institute of Japan. C-2, Structures IV, Reinforced Concrete Structures Prestressed Concrete Structures Masonry Wall Structures, 2005, 723–724*.
- NASA. (2005). Tsunami in the Indian Ocean: Tsunami Wave Height from Altimetry Data. Goddard Space Flight Center.
- National Police Agency of Japan. (2014). *Damage Situation and Police Countermeasures associated with 2011Tohoku district - off the Pacific Ocean Earthquake*. Emergency Disaster Countermeasures Headquarters. Retrieved from http://www.npa.go.jp/archive/keibi/biki/higaijokyo_e.pdf
- National Tsunami Hazard Mitigation Program. (2005). Tsunami Terminology. Retrieved from <http://nthmp-history.pmel.noaa.gov/terms.html>
- Ohmori, M., Fujii, N., & Kyotani, O. (2000). The numerical computation of the water level, the flow velocity and the wave force of the tsunami which overflow the perpendicular revetments. *Proceedings of the Coastal Engineerings of JSCE*, 47, 376–380.
- Okada, T., Sugano, T., Ishihara, T., Takai, S., & Tateno, T. (2006). Tsunami Loads and Structural Design of Tsunami Refugee Buildings. Building Technology Research Institute.

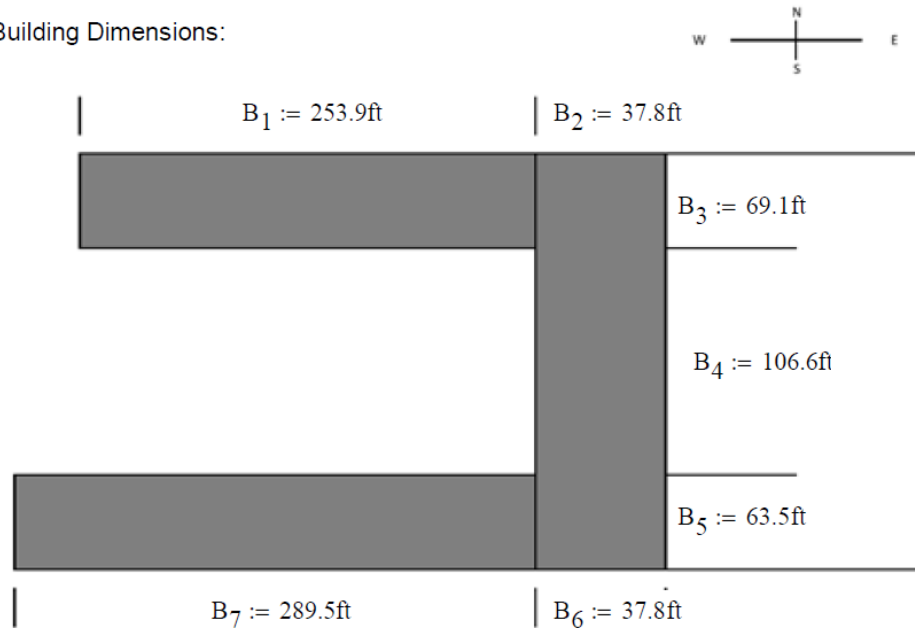
- Paczkowski, K., Riggs, R., & Robertson, I. (2011). Bore Impact upon Vertical Wall and Water-Driven, High-Mass, Low-Velocity Debris Impact, Research Report UHM/CEE/11-05. University of Hawaii. Retrieved from <http://www.cee.hawaii.edu/reports/UHM-CEE-11-05.pdf>
- Palermo, D., Nistor, I., Nouri, Y., & Cornett, A. (2009). Tsunami loading of near-shoreline structures: a primer. *Canadian Journal of Civil Engineering*, 36(11), 1804–1815. doi:10.1139/L09-104
- Peterson, K., & Naito, C. (2012). IMPACT FORCES FROM TSUNAMI-DRIVEN DEBRIS. Retrieved from http://nees.org/site/media/pdf/reu2011finalpapers/peterson_nees_reu_finalpaper.pdf
- Phillips, B., Neal, D., Wikle, T., Subanthore, A., & Hyrapiet, S. (2008). Mass fatality management after the Indian Ocean tsunami. *Disaster Prevention and Management*, 17(5), 681–697. doi:10.1108/09653560810918685
- Prasad, R. (2009). *Tsunami Hazard Assessment at Nuclear Power Plant Sites in the United States of America: Final Report*. US Nuclear Regulatory Commission, Office of New Reactors. Retrieved from <http://pbadupws.nrc.gov/docs/ML0915/ML091590193.pdf>
- Priest, G. R. (1995). *Explanation of mapping methods and use of the tsunami hazard maps of the Oregon coast*. State of Oregon, Dept. of Geology and Mineral Industries.
- Ramsden, J. (1993, May). *Tsunamis: Forces on a Vertical Wall Caused by Long Waves, Bores, and Surges on a Dry Bed*. California Institute of Technology, Pasadena, California.
- Raskin, J., Wang, Y., Boyer, M., Fiez, T., Moncada, J., Yu, K., & Yeh, H. (2011). An evacuation building project for Cascadia earthquakes and tsunamis. *Obras y Proyectos*, 9, 11–22.
- Santo, J., & Robertson, I. (2010). Lateral Loading on Vertical Structural Elements Due to a Tsunami Bore, Research Report UHM/CEE/10-02. University of Hawaii. Retrieved from <http://www.cee.hawaii.edu/reports/UHM-CEE-10-02.pdf>
- Shuto, N., & Fujima, K. (2009). A short history of tsunami research and countermeasures in Japan. *Proceedings of the Japan Academy, Series B*, 85(8), 267–275. doi:10.2183/pjab.85.267
- Tadepalli, S., & Synolakis, C. E. (1996). Model for the leading waves of tsunamis. *Physical Review Letters*, 77(10), 2141.
- The World Association for Waterborne Transport Infrastructure. (2010). Mitigation of Tsunami Disasters in Ports. PIANC.
- Thomson, R. E. (1981). *Oceanography of the British Columbia coast* (Vol. 56). Department of Fisheries and Oceans Sidney, BC. Retrieved from <http://www.getcited.org/pub/102256401>

- Titov, V. V., Gonzalez, F. I., Bernard, E. N., Eble, M. C., Mofjeld, H. O., Newman, J. C., & Venturato, A. J. (2005). Real-time tsunami forecasting: Challenges and solutions. In *Developing Tsunami-Resilient Communities* (pp. 41–58). Springer. Retrieved from http://link.springer.com/chapter/10.1007/1-4020-3607-8_3
- Titov, V. V., & Synolakis, C. E. (1998). Numerical modeling of tidal wave runup. *Journal of Waterway, Port, Coastal, and Ocean Engineering*, 124(4), 157–171.
- Togashi, H. (1986). Wave Force of Tsunami Bore on a Vertical Wall. Nagasaki University.
- Whitham, G. B. (1955). The Effects of Hydraulic Resistance in the Dam-Break Problem. *Proceedings of the Royal Society of London. Series A, Mathematical and Physical Sciences*, 227(1170), 399–407.
- Wigen, S. O., & White, W. R. H. (1964). *Tsunami of March 27-29, 1964: West Coast of Canada*. Department of Mines and Technical Surveys, Canada.
- World Bank, & GFDRR. (2012). Knowledge Notes. Retrieved from <https://www.eeri.org/projects/world-bank-and-global-facility-for-disaster-reduction-and-recovery-grant-agreement-2/>
- Yamazaki, F., & Zavala, C. (2013). SATREPS Project on Enhancement of Earthquake and Tsunami Disaster Mitigation Technology in Peru. *Journal of Disaster Research*, 8(2), 224–234.
- Yeh, H. (1998). Tsunami researchers outline steps for better data. *Eos, Transactions American Geophysical Union*, 79(40), 480–484.
- Yeh, H. (2007). Design Tsunami Forces for Onshore Structures. *Journal of Disaster Research*, Vol.2, No.6.
- Yeh, H. (2009). Tsunami Impacts on Coastlines. In *Tsunamis* (Vol. 15, pp. 333–369). Harvard University Press.
- Yeh, H., Liu, P., Briggs, M., & Synolakis, C. (1994). Propagation and amplification of tsunamis at coastal boundaries. *Nature*, 372(6504), 353–355.
- Yeh, H., & Mason, H. B. (2014). Sediment response to tsunami loading: mechanisms and estimates. *Géotechnique*, 64(2), 131–143. doi:10.1680/geot.13.P.033
- Yeh, H., Robertson, I., & Preuss, J. (2005). *Development of design guidelines for structures that serve as tsunami vertical evacuation sites*. Washington State Dept. of Natural Resources, Division of Geology and Earth Resources. Retrieved from http://nctr.pmel.noaa.gov/tsu400/documents/Course_3_Day_3/Session_8/ofr05-4.pdf
- Yeh, H., Sato, S., & Tajima, Y. (2013). The 11 March 2011 East Japan Earthquake and Tsunami: Tsunami Effects on Coastal Infrastructure and Buildings. *Pure and Applied Geophysics*, 170(6), 1019–1031. doi:10.1007/s00024-012-0489-1

APPENDIX

Given:

Building Dimensions:



$$B := B_3 + B_4 + B_5 = 72.908 \text{ m}$$

Density of Fluid Including Sediments: $\rho := 1100 \frac{\text{kg}}{\text{m}^3}$

Acceleration due to gravity $g := 9.81 \frac{\text{m}}{\text{s}^2}$

Coefficient of Drag $C_d := 2$

Given: Tier 1 Inundation Parameters

Maximum Inundation Depth $h_{\text{max}} := 2.5 \text{ m}$

Elevation of Site $z := 23 \text{ ft} = 7.01 \text{ m}$

Maximum Elevation of Runup $R := z + h_{\text{max}} = 10 \text{ m}$

Factored Maximum Elevation of Runup $R_{\text{f}} := R \cdot 130\% = 12.364 \text{ m}$

Maximum Momentum Flux $\text{maxmomentumflux} := g \cdot R^2 \cdot \left[0.125 - 0.235 \cdot \left(\frac{z}{R} \right) + 0.11 \cdot \left(\frac{z}{R} \right)^2 \right] = 10.243 \frac{\text{m}^3}{\text{s}^2}$

Factored Maximum Momentum Flux $\text{maxmomentumflux} := 170\% \cdot \left[g \cdot R^2 \cdot \left[0.125 - 0.235 \cdot \left(\frac{z}{R} \right) + 0.11 \cdot \left(\frac{z}{R} \right)^2 \right] \right] = 17.413 \frac{\text{m}^3}{\text{s}^2}$

Tier 1 Analysis

Find:

Hydrostatic Force:

$$F_H(b) := \frac{1}{2} \cdot \rho \cdot g \cdot b \cdot h_{\max}^2$$

Hydrodynamic Force:

$$F_d := \frac{1}{2} \cdot \rho \cdot C_d \cdot B \cdot \text{maxmomentumflux}$$

Impulsive Force:

$$F_I := 1.5 \cdot F_d$$

Solution:

Hydrostatic Force:

E/W:

N/S:

$$F_H(B_4) = 246 \cdot \text{kip}$$

$$F_H(B_1) = 587 \cdot \text{kip}$$

$$F_H(B_5) = 147 \cdot \text{kip}$$

$$F_H(B_7) = 669 \cdot \text{kip}$$

Hydrodynamic Force:

$$F_d = 314 \cdot \text{kip}$$

Impulsive Force:

$$F_I = 471 \cdot \text{kip}$$

Total Force: (Asakura, 2002) $\alpha := 3$

$$F_H := \frac{1}{2} \cdot \rho \cdot g \cdot B \cdot (\alpha \cdot h_{\max})^2 = 4974 \cdot \text{kip}$$

$$F_H := \frac{1}{2} \cdot \rho \cdot g \cdot B \cdot (\alpha \cdot h_{\max})^2 = 4974 \cdot \text{kip}$$

Tier 2 Analysis

Given: Tier 2 Inundation Parameters

Maximum Inundation Depth

$$h_{\max} := 2.5\text{m}$$

Factored Maximum Inundation Depth

$$h_{\max} := 2.5\text{m} \cdot 130\% = 3.25\text{m}$$

Maximum Velocity

$$u_{\max} := 7.5 \frac{\text{m}}{\text{s}}$$

Factored Maximum Velocity

$$u_{\max_} := 115\% \cdot u_{\max} = 8.625 \frac{\text{m}}{\text{s}}$$

Factored Maximum Momentum Flux

$$\text{maxmomentumflux} := 140 \frac{\text{m}^3}{\text{s}^2} \cdot 170\% = 238 \frac{\text{m}^3}{\text{s}^2}$$

Density of Fluid
Including Sediments

$$\rho := 1100 \frac{\text{kg}}{\text{m}^3}$$

Acceleration due to gravity

$$g := 9.81 \frac{\text{m}}{\text{s}^2}$$

Coefficient of Drag

$$C_d := 2$$

Find:

Hydrostatic Force:

$$F_H(b) := \frac{1}{2} \cdot \rho \cdot g \cdot b \cdot h_{\max}^2$$

Hydrodynamic Force:

$$F_d := \frac{1}{2} \cdot \rho \cdot C_d \cdot B \cdot \text{maxmomentumflux}$$

Impulsive Force:

$$F_I := 1.5 \cdot F_d$$

Solution:

Hydrostatic Force:

E/W:

N/S:

$$F_H(B_4) = 416 \cdot \text{kip}$$

$$F_H(B_1) = 991 \cdot \text{kip}$$

$$F_H(B_5) = 248 \cdot \text{kip}$$

$$F_H(B_7) = 1131 \cdot \text{kip}$$

Hydrodynamic Force:

$$F_d = 4291 \cdot \text{kip}$$

Impulsive Force:

$$F_I = 6437 \cdot \text{kip}$$